



---

# DET NORSKE VERITAS

---

## Final Report Feasibility Evaluation of Chemical Inhibition of Ethanol SCC

Pipeline & Hazardous Materials Safety Administration  
U.S. Department of Transportation  
Washington, DC

Report No./DNV Reg No.: 2012-9192




March 28, 2012



Feasibility Evaluation of Chemical Inhibition of Ethanol SCC	DET NORSKE VERITAS (U.S.A.), INC. Materials & Corrosion Technology Center 5777 Frantz Road Dublin, OH 43017-1386, United States Tel: (614) 761-1214 Fax: (614) 761-1633 <a href="http://www.dnv.com">http://www.dnv.com</a> <a href="http://www.dnvcolumbus.com">http://www.dnvcolumbus.com</a>
For:	
Pipeline & Hazardous Materials Safety Administration U.S. Department of Transportation East Building, 2 <sup>nd</sup> Floor 1200 New Jersey Ave., SE Washington, DC 20590	
Account Ref.:	

Date of First Issue:	March 28, 2012	Project No.	EP021141
Report No.:	2012-9192	Organization Unit:	DNV Research & Innovation
Revision No.:	0	Subject Group:	

Summary:
See Executive Summary

Prepared by:	Feng Gui, Ph.D. Senior Engineer	Signature 
Verified by:	Narasi Sridhar, Ph.D. Director – Program Director Materials and Sensors Program	Signature 
Approved by:	Narasi Sridhar, Ph.D. Director – Program Director Materials and Sensors Program	Signature 

<input checked="" type="checkbox"/>	No distribution without permission from the client or responsible organizational unit (however, free distribution for internal use within DNV after 3 years)	Indexing Terms	
<input type="checkbox"/>	No distribution without permission from the client or responsible organizational unit	Key Words	
<input type="checkbox"/>	Strictly confidential	Service Area	
<input type="checkbox"/>	Unrestricted distribution	Market Segment	

Rev. No. / Date:	Reason for Issue:	Prepared by:	Approved by:	Verified by

© 2011 Det Norske Veritas (U.S.A.), Inc.  
All rights reserved. This publication or parts thereof may not be reproduced or transmitted in any form or by any means, including photocopying or recording, without the prior written consent of Det Norske Veritas (U.S.A.), Inc.

## Executive Summary

Stress corrosion cracking (SCC) has been observed in carbon steel tanks and piping in contact with fuel grade ethanol (FGE) in user terminals, storage tanks, and loading/unloading racks. Detailed laboratory studies, sponsored by American Petroleum Institute (API), Renewable Fuel Association (RFA), Pipeline Research Council International (PRCI), and Pipeline and Hazardous Materials and Safety Administration (PHMSA), demonstrated that, in ASTM D-4806 FGE, dissolved oxygen was the most important factor leading to SCC, followed in importance by pre-existing scale on the steel, chloride, and methanol. In a Roadmapping Workshop conducted in October 2007, methods to avoid oxygen contamination in ethanol and defining safe operating limits in terms of ethanol chemistry and oxygen concentration were identified as major gaps in the safe transportation of ethanol in pipelines.

Using inhibitors to prevent SCC in FGE is a possible solution, but the impact on the fuel end use applications needs to be considered. The ability of the inhibitors to prevent SCC was evaluated under flowing conditions created by jet impingement, which is believed to simulate pipe flow in the pipelines. The results established the baseline for inhibitor performance in mitigating carbon steel SCC and provided insights in the feasibility of SCC prevention by chemical addition. Furthermore, an electrochemical method was developed for rapid evaluation of inhibitors in FGE. This method was supported by the understanding of the oxygen role in promoting SCC and the mechanistic study performed in this work and in previous projects.

The present project continued to address the gaps remained after the PRCI SCC 4-3 Phase II:

- The crack growth tests under flowing condition are to be performed to determine whether the inhibitors would perform similarly in flowing solution similar to that would be encountered in transmission pipeline.
- A rapid method to select inhibitor for carbon steel SCC mitigation is still to be developed.
- Among the inhibitors that were demonstrated effective in mitigating carbon SCC in FGE, it would be beneficial to know if they would perform well below currently used dosage.

The objectives of the project were:

- Evaluate the performance of selected inhibitors in long term crack growth experiments under flowing conditions simulated by jet impingement.
- Develop a method to rapidly evaluate and select SCC inhibitors for use in FGE.
- Evaluate the feasibility of chemical inhibition of carbon steel SCC in FGE

The following tests were performed to achieve the above objectives:



- Crack growth rate (CGR) test under flowing conditions to evaluate inhibitor performance in SFGE and FGE.
- CGR test in SFGE, E50 and FGE to evaluate the threshold concentration of inhibitors.
- CGR test in SFGE to evaluate the threshold oxygen concentration beyond which cracking would occur on carbon steel.
- Electrochemical tests to develop a rapid inhibitor screening method.
- Electrochemical tests to further provide insights in the SCC mechanism of carbon steel in SFGE which in turn would provide guideline on the development of a rapid method to select inhibitor to mitigate carbon steel SCC in FGE.

Based on the performed tests, these are the key results:

- Commercially available inhibitors or generic chemicals (such as  $\text{NH}_4\text{OH}$ ) selected for use in this work were all demonstrated to be able to mitigate the propagating crack in SFGE, FGE and E50;
- Ammonium hydroxide was the most effective inhibitor but the addition of a minimum effective concentration would result in a pHe of ~9 that is the upper bound of the current fuel specification;
- Although some commercial inhibitors tested in this work can mitigate SCC in E50, substantially higher concentration is needed compared to when  $\text{NH}_4\text{OH}$  was used;
- The performance of those inhibitors shown to be effective in stagnant solution remains the same under flowing condition that mimics the turbulent pipe flow;
- Electrochemical technique was able to provide fast screening of inhibitors for a specific application before confirmed by CGR tests; the results from the study of the role of oxygen and carbon steel SCC mechanism support this statement;
- Chemical inhibition of carbon steel SCC in FGE is a viable option based on the obtained results. The industry has established the inhibitor injection practice to control general corrosion; such practice can be easily extended to SCC control;

The results obtained in this project and another SCC prevention feasibility evaluation project (WP#384) will be communicated to NACE Biofuel Task Group. It is expected these results will serve as the foundation for developing guidelines and standard testing methodologies to select and apply inhibitors for mitigating carbon steel SCC in FGE.



## Recommendations

- The effect of recommended SCC inhibitors on automotive components needs to be investigated. Note that the corrosion inhibitors that are recommended for ethanol service are not effective inhibitors of SCC.



## Table of Contents

1.0	BACKGROUND .....	9
2.0	SUMMARY OF PRCI SCC 4-3 PHASE 2 .....	10
3.0	REMAINED GAP .....	14
4.0	OBJECTIVES .....	14
5.0	PROJECT SCOPE .....	15
6.0	EXPERIMENTAL APPROACH .....	15
6.1	Testing environment .....	15
6.2	Crack Growth Rate Test under Flowing Condition .....	16
6.3	<u>Electrochemical Studies to Develop Rapid Selection Method for Inhibitor</u> .....	22
7.0	RESULTS .....	26
7.1	<u>Task 1: Inhibitor Performance Evaluation</u> .....	26
7.1.1	Inhibitor performance under flowing conditions .....	26
7.1.2	Threshold concentration evaluation .....	31
7.1.3	Threshold oxygen concentration evaluation .....	39
7.2	<u>Task 2: Rapid Inhibitor Selection Method</u> .....	41
7.2.1	Electrochemical behavior of carbon steel in inhibited SFGE .....	41
7.2.2	Crevice corrosion of carbon steel in SFGE .....	44
7.3	<u>Task 3: Feasibility Evaluation</u> .....	53
8.0	SUMMARY .....	54
	APPENDIX: CGR TESTS SUMMARY TABLE .....	55



## List of Tables

Table 1. Target composition of SFGE. ....	16
Table 2. Tested inhibitors .....	16
Table 3. Solution pH change with different concentrations of $\text{NH}_4\text{OH}$ . ....	33

## List of Figures

Figure 1. Schematic of compact tension specimen.....	18
Figure 2. Photograph of the inside of the test cell used for crack-growth testing, showing the test specimen and cell internals; RCS –Rusted Carbon Steel Sample, EPD – Electric Potential Drop.....	19
Figure 3. Hydrodynamic characteristics of jet impingement on a flat plate showing the four characteristic flow regions . ....	20
Figure 4. Jet impingement setup to create flowing conditions on the CT sample .....	22
Figure 5. Illustrations of the electrochemical experimental setup (a) and the test cell (b). ....	24
Figure 6. Electrode array embedded in a carbon steel cylinder.....	25
Figure 7. Illustration of the crevice assembly.....	25
<b>Figure 8. Crack length as a function of time for Base-17 under flowing SFGE to evaluate Inhibitor A. ....</b>	<b>27</b>
Figure 9. Crack length as a function of time for Base-17 under flowing SFGE to evaluate Inhibitor C. ....	28
<b>Figure 10. Crack length as a function of time for Base-17 under flowing SFGE to evaluate INHIBITOR B.....</b>	<b>29</b>
<b>Figure 11. Crack length as a function of time for Base-17 under flowing FGE to evaluate INHIBITOR B. ....</b>	<b>30</b>
<b>Figure 12. Crack length change as a function of time for sample Base-9 to evaluate the threshold concentration of Inhibitor A in SFGE. ....</b>	<b>31</b>
<b>Figure 13. Crack length change as a function of time for sample Base-10 to evaluate the threshold concentration of Inhibitor C. ....</b>	<b>32</b>
<b>Figure 14. Crack length change as a function of time for sample Base-11 to evaluate the threshold concentration of INHIBITOR B in SFGE. ....</b>	<b>33</b>
<b>Figure 15. Crack length change as a function of time for sample Base-10 to evaluate the threshold concentration of NH<sub>4</sub>OH in SFGE. ....</b>	<b>34</b>
<b>Figure 16. Crack length change as a function of time for samples HAZ-2 and Base-9 to evaluate the threshold concentration of Inhibitor A in E50. ....</b>	<b>35</b>
<b>Figure 17. Crack length change as a function of time for sample Base-15 to evaluate the threshold concentration of INHIBITOR B in E50.....</b>	<b>36</b>





<b>Figure 18. Crack length change as a function of time for sample HAZ-2 to evaluate the threshold concentration of <math>\text{NH}_4\text{OH}</math> in E50.</b>	37
<b>Figure 19. Crack length change as a function of time for samples Base-11 and Base-12 to evaluate the threshold concentration of <math>\text{NH}_4\text{OH}</math> in FGE.</b>	38
<b>Figure 20. Crack length as a function of time for Base-11 sample to evaluate the threshold oxygen concentration for cracking.</b>	39
<b>Figure 21. Crack length as a function of time for Base-18 sample to evaluate the threshold oxygen concentration for cracking.</b>	40
Figure 22: Comparison of polarization curves of carbon steel in SFGE containing an inhibitor that was effective in mitigating SCC (a) and an inhibitor that was not effective in mitigating SCC (b).	42
<b>Figure 23: Crack length and growth rate as a function of time before and after inhibitors were injected.</b>	43
Figure 24. Current map of the array after one week of exposure at OCP in SFGE. (a) deaerated; (b) aerated (Unit: A)	44
Figure 25. Comparison of the current as a function for electrode (3, 11) that locates near the crevice mouth.	45
Figure 26. Depth of attack on the electrode array after one week of immersion in SFGE at OCP . (a) deaerated; (b) aerated	46
Figure 27. Current map (a) and depth of attack for the electrode array after approximately 90 hours immersion in deaerated SFGE with 0.02 M TBA-TFB as the supporting electrolyte.	48
Figure 28. Depth of attack for the array with tighter gap exposed in deaerated SFGE for one week.	49
Figure 29. Current map (a) and the depth of attack for the array after one week of exposure at OCP in SFGE purged with 1% oxygen	50
Figure 30. Current of the electrode (10, 3) at the crevice mouth and the electrode potential as a function of time in the test when the purging gas was switched from nitrogen to air. The current maps at three different points on the current of the electrode (10, 3) are shown.	53



## 1.0 BACKGROUND

Ethanol has attracted much attention in recent years as an alternative fuel source in an effort to improve security of supply and energy independence. In the US, the US Department of Energy (DOE) calls for 30% of today's fuel use to be supplanted by 2030 with alternate fuels, including ethanol<sup>\*</sup>. Worldwide, ethanol demand is expected to more than double in the next ten years<sup>†</sup>. Although most of the ethanol is currently transported by tanker trucks, rail cars, and barges, pipelines are still the most efficient system to transport ethanol. Thus, with increases in ethanol demand, it is expected that pipelines - both the existing pipeline infrastructure and new pipeline construction - will play a major role in transporting ethanol.

Stress corrosion cracking (SCC) has been observed in carbon steel tanks and piping in contact with fuel grade ethanol (FGE) in user terminals, storage tanks, and loading/unloading racks. Detailed laboratory studies<sup>‡</sup>, sponsored by American Petroleum Institute (API), Renewable Fuel Association (RFA), Pipeline Research Council International (PRCI), and Pipeline and Hazardous Materials and Safety Administration (PHMSA), demonstrated that, in ASTM D-4806 FGE, dissolved oxygen was the most important factor leading to SCC, followed in importance by pre-existing scale on steel, chloride, and methanol. In a Roadmapping Workshop conducted in October 2007<sup>§</sup>, methods to avoid oxygen contamination in ethanol and defining safe operating limits in terms of ethanol chemistry and oxygen concentration were identified as major gaps in the safe transportation of ethanol in pipelines.

Corrosion inhibitors, such as Octel DCI-11, that are commonly used to prevent general corrosion in ethanol service are not effective in mitigating SCC. Using other inhibitors to prevent SCC in FGE is unique in that extra steps need to be taken on the inhibitor selection because the impact on the fuel end users needs to be considered. This project combined the effort from the inhibitor manufacturers and pipeline operators with an attempt to select inhibitors that can potentially prevent SCC and are acceptable based on technical and end user compatibility considerations. More importantly, the ability of the inhibitors to prevent SCC was evaluated under flowing conditions created by jet impingement, which is believed to simulate pipe flow in the pipelines. The results will help identify the appropriate inhibitors, the optimum dosage and guide the application of inhibitors (e.g. batch vs. continuous) in operations. Furthermore, a method was developed for rapid evaluation of inhibitors in FGE. Such a method will be essential and useful when new inhibitors are considered or existing operation conditions are changed so that either

---

<sup>\*</sup> C. Schubert, Nature Biotechnology, 24, 777 (2006).

<sup>†</sup> M. F. Demirbas and M. Balat, Energy Conversion and Management, 47, 2371 (2006).

<sup>‡</sup> N. Sridhar, K. Price, J. Buckingham and J. Dante, "Stress Corrosion Cracking of Carbon Steel in Ethanol", Corrosion, v62, 8 (2006):p687

<sup>§</sup> Safe & Reliable Ethanol Transportation & Storage Technology Roadmapping Workshop, October 25-27, 2007, Dublin, OH, Report prepared by DNV Columbus and Energetics.

the efficacy of different inhibitors or different concentration of the same inhibitors needs to be evaluated.

## 2.0 SUMMARY OF PRCI SCC 4-3 PHASE 2

This project is a continuation of the PRCI SCC 4-3 Phase 2 that was completed in 2010\*. The key results of the PRCI SCC 4-3 Phase 2 are summarized below.

The Phase 2 program under SCC 4-3 further addressed Gap 4 from the 2007 Roadmapping Workshop.

Gap 4: The implementation of various SCC mitigation methods in the field had not been developed. For example, the effectiveness of oxygen scavengers may depend on dosage, introduction mode, gas/liquid phase ratio, flow rate, presence of solids, residence time, long line effect/topography, etc.

A project in response to PHMSA solicitation DTRS56-07-0002 addresses many of the remaining gaps with the ultimate goal of integrating the results of all planned efforts to develop a coherent methodology for sound decision-making regarding reliable and safe transportation of ethanol in pipelines.

The primary objective of Phase 2 of SCC 4-3 was to determine if inhibitors are effective in preventing stress corrosion crack growth under more realistic field conditions than those found in the SSR tests performed to date.

The original proposed Phase 2 scope of work consisted of three tasks: Task 1 – Crack Growth Tests Under Flowing Conditions, Task 2 – Electrochemical/Corrosion Tests, and Task 3 – Reporting and Project Management. This scope was changed shortly after initiating the project based on input from PRCI. The work was focused on screening of commercial SCC inhibitors. This necessitated adding a task in which the inhibitors were initially screened using the SSR technique. The best performing inhibitors were then evaluated using the more realistic crack growth tests. The crack growth tests under flowing conditions (Task 1) and the electrochemical/corrosion tests (Task 2) were deferred to the PHMSA portion of the consolidated program.

The modified scope consisted of three tasks:

### Task 1 – Inhibitor Screening Tests

---

\* John Beavers, Feng Gui, Narasi Sridhar, "Identify Environmental and Stress Factors that Produce SCC in Existing Ethanol Pipelines and Terminals", PRCI Final Report (Contract# PR186-073508).

## Task 2 – Crack Growth Tests, and

## Task 3 – Reporting and Project Management.

Two types of SCC tests were performed in the Phase 2 research: SSR tests and crack growth tests. The majority of the research was performed using the SFGE. This was done to avoid experimental difficulties associated with degradation or changes in the FGE.

In Task 1, the SSR test technique was used as a screening tool to evaluate commercial inhibitors. In this test, the specimen is slowly strained to failure in the cracking environment. SCC susceptibility is indicated by a decrease in the mechanical properties, over those observed in air, and the presence of thumbnail cracks on the fracture surface. In the case of un-notched tensile specimens, SCC susceptibility also is indicated by the presence of secondary cracks on the gage section of the specimen. The inhibitors were added to the SFGE prior to testing, at the concentration specified by the commercial supplier. The best performing inhibitors were selected for the more realistic long-term crack growth tests in Task 2. Slow strain rate tests also were performed to evaluate the effect of environmental factors (e.g., oxygen, blend ratio, non-commercial inhibitors) on SCC behavior.

The majority of SSR tests were performed with un-notched specimens machined from the base metal of one vintage 1978 API 5L X60 line-pipe steel in the axial orientation. A few SSR tests were performed with notched specimens machined from the base metal of one vintage 1963 API 5L X 46 line pipe steel in the axial orientation. Prior research has shown that there is little or no difference in the susceptibility of different pipe steels to ethanol SCC.

After testing, the specimens were examined and optically photographed. The fracture surfaces were examined in the scanning electron microscope (SEM) and the maximum depth of SCC was measured. Other parameters that were recorded for each test included the maximum load and the time to failure.

As previously described, the better performing inhibitors identified in Task 1 were tested in long-term crack growth tests in Task 2. These tests were performed on base metal specimens machined from the X 46 line pipe steel. This is the same steel used for the SSR tests with notched specimens, in Task 1.

The crack growth tests were performed using fatigue precracked 1/2T compact type (CT) tests specimens. The use of a pre-cracked, CT specimen geometry is justified because of the likely presence of undetected flaws in pipelines. The specimens were oriented such that the through-wall pre-crack propagated in the axial pipe direction. Fatigue pre-cracking was performed using a load shedding technique to minimize the plastic zone size.

The crack growth in the tests was monitored continuously using an electric potential drop (EPD) technique in accordance with the procedures found in ASTM E647-00. With this technique, a direct current of 20 amperes was passed through the specimen and the change in resistance of the specimen, as a result of crack extension, was monitored. Further details on the procedures, accuracy, and limitations of the technique can be found in the ASTM standard.

The tests were performed under cyclic loading conditions. These load conditions are designed to simulate the loading conditions on a just - surviving crack in a pipeline that had been previously hydrostatically tested. The imposition of a cyclic load is important since it produces continuous micro-plastic deformation at the crack tip that enhances SCC growth and simulates the ripple load effect from pressure fluctuations on an operating pipeline. The ratio of the minimum to maximum load (R ratio) in the tests ranged from 0.6 to 0.8 and the cyclic frequency was  $1.2 \times 10^{-4}$  Hz (one cycle every 2.3 hours). These conditions are typical of cyclic pressure fluctuations on liquid petroleum pipelines. For each specimen, cracking was initiated in the SFGE and propagated for approximately a one-month period. The inhibitor was then added to the test cell and the effect of the inhibitor on subsequent crack growth was evaluated. Several tests also were performed to evaluate the effect of other environmental factors on SCC crack growth. Control tests also were performed in air under the same cyclic loading conditions. Negligible crack growth was observed, demonstrating that fatigue crack growth was negligible in these tests.

Over 20 commercial inhibitors and several potential non-commercial inhibitors, including ammonium hydroxide, were evaluated in this research. Some commercial inhibitors were effective in inhibiting ethanol SCC under many of the test conditions. The commercial inhibitors, in general, were less effective in E-50 than in SFGE. One commercial inhibitor also was less effective in one lot of corn-based FGE than in SFGE. Ammonium hydroxide, at a relatively low concentration, was, by far, the most effective inhibitor evaluated.

In addition, a number of environmental factors were evaluated including the effects of oxygen, chloride, water, blends, ethanol source (SFGE vs. wet milled corn-based FGE), and batching. In agreement with all of the previous research, complete removal of oxygen arrested cracking. While E-50 did not appear to be significantly more potent in the un-notched SSR tests, much higher crack growth rates were observed in E-50, compared with SFGE, in the crack growth tests. In this aggressive E-50 environment, the inhibitors were generally less effective. It also was observed that water additions, >4.5 %, or the removal of chloride additions to the SFGE did not completely inhibit cracking in the crack growth tests. These changes eliminated SCC in the un-notched SSR tests. This behavior indicates that the crack growth tests are somewhat more aggressive than the un-notched SSR tests.

There were a number of interesting findings related to the test techniques. In the inhibitor studies, the results of un-notched SSR tests generally correlated well with results of crack growth tests using pre-cracked CT specimens. On the other hand, the notched SSR test technique is



much more aggressive. For example, severe SCC was observed in a SSR test with a notched specimen in SFGE containing 150 ppm  $\text{NH}_4\text{OH}$ ; whereas, no SCC was observed under similar test conditions with an un-notched specimen. Furthermore, 150 ppm  $\text{NH}_4\text{OH}$  consistently arrested cracking in the crack growth tests, even in the presence of the more potent E-50 environment. It is the opinion of the authors that, of these three types of SCC tests, the crack growth tests are the most realistic of field conditions. Accordingly, these observations indicate that the notched SSR test technique is so aggressive that it is not useful for screening inhibitors.

The following are the conclusions of Phase 2 of SCC 4-3:

The un-notched SSR test results generally correlated well with the results of the crack growth tests using pre-cracked CT specimens, although the latter test technique was somewhat more aggressive.

The SSR test technique with notched specimens was more aggressive than that with un-notched specimens and did not correlate well with the crack growth tests.

In the crack growth tests, E-50, prepared with SFGE, was consistently more potent as a cracking agent than SFGE.

Some commercial inhibitors were effective in inhibiting ethanol SCC under many of the test conditions.

The commercial inhibitors, in general, were less effective in E-50 than in SFGE.

Ammonium hydroxide, at a relatively low concentration, was by far the most effective inhibitor evaluated.

For one commercial inhibitor, a higher concentration was needed to inhibit SCC in one lot of corn based FGE than in SFGE.

Water inhibited, but did not completely arrest, SCC in the crack growth tests in SFGE.

Sustained crack growth was observed in SFGE in which no chloride was added.

Evidence of loss of inhibition, at low concentrations, was observed in an inhibition scheme for batching of FGE with gasoline in which a high initial dose, followed by a low maintenance dose was used.

One significant implication of the research results is that SCC inhibitors should be evaluated in the specific ethanol/ blend and dosing scheme in which they will be used. Some commercial inhibitors were effective in inhibiting ethanol SCC under many of the test conditions. However, they generally were less effective in E-50 than in SFGE. One commercial inhibitor also was less effective in a lot of corn-based FGE than in SFGE. Evidence of loss of inhibition, at low





concentrations, was observed with this inhibitor in a scheme for batching of FGE with gasoline in which a high initial dose, followed by a low maintenance dose was used.

Ammonium hydroxide, at a relatively low concentration, was by far the most effective inhibitor evaluated. It effectively inhibited SCC under conditions in which the commercial inhibitors were either ineffective and or required higher concentrations for inhibition. However, the compatibility of ammonium hydroxide with downstream components and corrosion inhibitors and other additives for ethanol or gasoline has not been investigated.

Another implication of the research is that the notched SSR test technique is so aggressive that it is not useful for screening inhibitors. Results using the technique did not correlate well with results of crack growth tests or results of un-notched SSR tests. Inhibitors that were effective in the latter two techniques such as  $\text{NH}_4\text{OH}$ , did not inhibit cracking in notched SSR tests.

The work planned in the original scope of SCC 4-3 Phase 2 should be completed. The electrochemical tests will provide a better understanding of the mechanisms of corrosion and SCC in FGE. The SCC tests under flowing conditions should be completed to demonstrate that inhibitor effectiveness is not degraded under realistic flowing conditions in an operating pipeline.

### 3.0 REMAINED GAP

Although further knowledge was gained in the PRCI SCC 4-3 Phase II project on the inhibitors with respect to their efficacy in mitigating carbon SCC in FGE, several gaps still remain:

1. As mentioned in the summary of the PRCI project above, the crack growth tests under flowing condition are to be performed to determine whether the inhibitors would perform similarly in flowing solution similar to that would be encountered in transmission pipeline.
2. A rapid method to select inhibitor for carbon steel SCC mitigation is still to be developed.
3. Among the inhibitors that were demonstrated effective in mitigating carbon SCC in FGE, it would be beneficial to know if they would perform well below currently used dosage.

This work aims to fill in these gaps.

### 4.0 OBJECTIVES

The major objectives of the proposed project were to:



1. Evaluate the performance of selected inhibitors in long term crack growth experiments under flowing conditions simulated by jet impingement.
2. Develop a method to rapidly evaluate and select SCC inhibitors for use in FGE.
3. Evaluate the feasibility of chemical inhibition of carbon steel SCC in FGE

## 5.0 PROJECT SCOPE

To achieve the objectives of the projects, the following tests were performed:

1. Crack growth rate (CGR) test under flowing conditions to evaluate inhibitor performance in SFGE and FGE.
2. CGR test in SFGE, E50 and FGE to evaluate the threshold concentration of inhibitors.
3. CGR test in SFGE to evaluate the threshold oxygen concentration beyond which cracking would occur on carbon steel.
4. Electrochemical tests to develop a rapid inhibitor screening method.
5. Electrochemical tests to further provide insights in the SCC mechanism of carbon steel in SFGE which in turn would provide guideline on the development of a rapid method to select inhibitor to mitigate carbon steel SCC in FGE.

The results are summarized in the following sections.

## 6.0 EXPERIMENTAL APPROACH

### 6.1 Testing environment

Most tests in this work were performed in SFGE. The SFGE was prepared with 200-proof ethanol and contaminants and additions found in the ASTM standard D4806<sup>\*</sup> with the composition listed in Table 1. The SFGE prepared following this procedure is referred as E95 in this report. The SFGE was also diluted with gasoline to obtained E50.

---

<sup>\*</sup> ASTM D4806-01a, "Standard Specification for Denatured Fuel Ethanol for Blending with Gasoline for Use as Automotive Spark-Ignition Engine Fuel", ASTM International (West Conshohocken, PA).



**Table 1. Target composition of SFGE.**

Requirement	ASTM Limits	
	Min.	Max.
Ethanol, vol. %	92.1	–
Methanol, vol. %	–	0.5
Solvent-washed gum, mg/100 ml	–	5.0
Water content, vol. %	–	1.0
Denaturant content, vol. %	1.96	5.00
Inorganic chloride, ppm (mg/L)	–	5
Copper, mg/kg	–	0.1
Acidity (as Acetic Acid CH <sub>3</sub> COOH), mass % (mg/L)	–	0.007 (56)
pH <sub>e</sub>	6.5	9.0

A FGE lot was also used in the CGR test to evaluate the performance of an inhibitor. This FGE was supplied by ADM for a PHMSA project previously executed at DNV (#WP323).

The inhibitors listed in Table 2 that were demonstrated effective in the PRCI SCC 4-3 Phase II project were further evaluated in this work.

**Table 2. Tested inhibitors**

Inhibitor label	Standard dosage (ppm)
Inhibitor A	250
Inhibitor B	500
Inhibitor C	3156
NH <sub>4</sub> OH	37.5 (added as 30 wt% aqueous solution)

All inhibitors were evaluated using jet impingement crack growth rate tests to evaluate their performance under flowing SFGE and FGE. Selected inhibitors were also evaluated in stagnant solutions (SFGE, FGE and E50) to investigate their threshold concentration for SCC mitigation. The objective of these threshold concentration evaluations was to explore if SCC can be mitigated at a lower concentration than that listed in Table 2.

## 6.2 Crack Growth Rate Test under Flowing Condition

The experimental approach for crack growth rate measurement is similar to that was used in PRCI SCC-4-4/PHMSA # 325. Fatigue pre-cracked compact tension specimens were exposed to FGE with and without added inhibitors under freely corroding conditions, and a cyclic load was applied to the specimens using a modified creep frame. Crack growth was monitored using an



electric potential drop technique. The test was performed on 1/2T compact tension specimen (see Figure 1 and Figure 2) under cyclic loading conditions. The samples were machined from the base metal of one vintage 1978 API 5L X60 line-pipe steel. These load conditions are designed to simulate the loading conditions on a just-surviving crack in a pipeline that has been previously hydrostatically tested. The imposition of a cyclic load is important since it produces continuous micro-plastic deformation that enhances SCC growth and simulates the ripple load effect from pressure fluctuations on an operating pipeline. The ratio of the minimum to maximum load (R ratio) in the tests ranged from 0.6 to 0.8 and the cyclic frequency was  $1.4 \times 10^{-4}$  Hz (one cycle every 2.8 hours). These conditions are typical of cyclic pressure fluctuations on liquid petroleum pipelines.

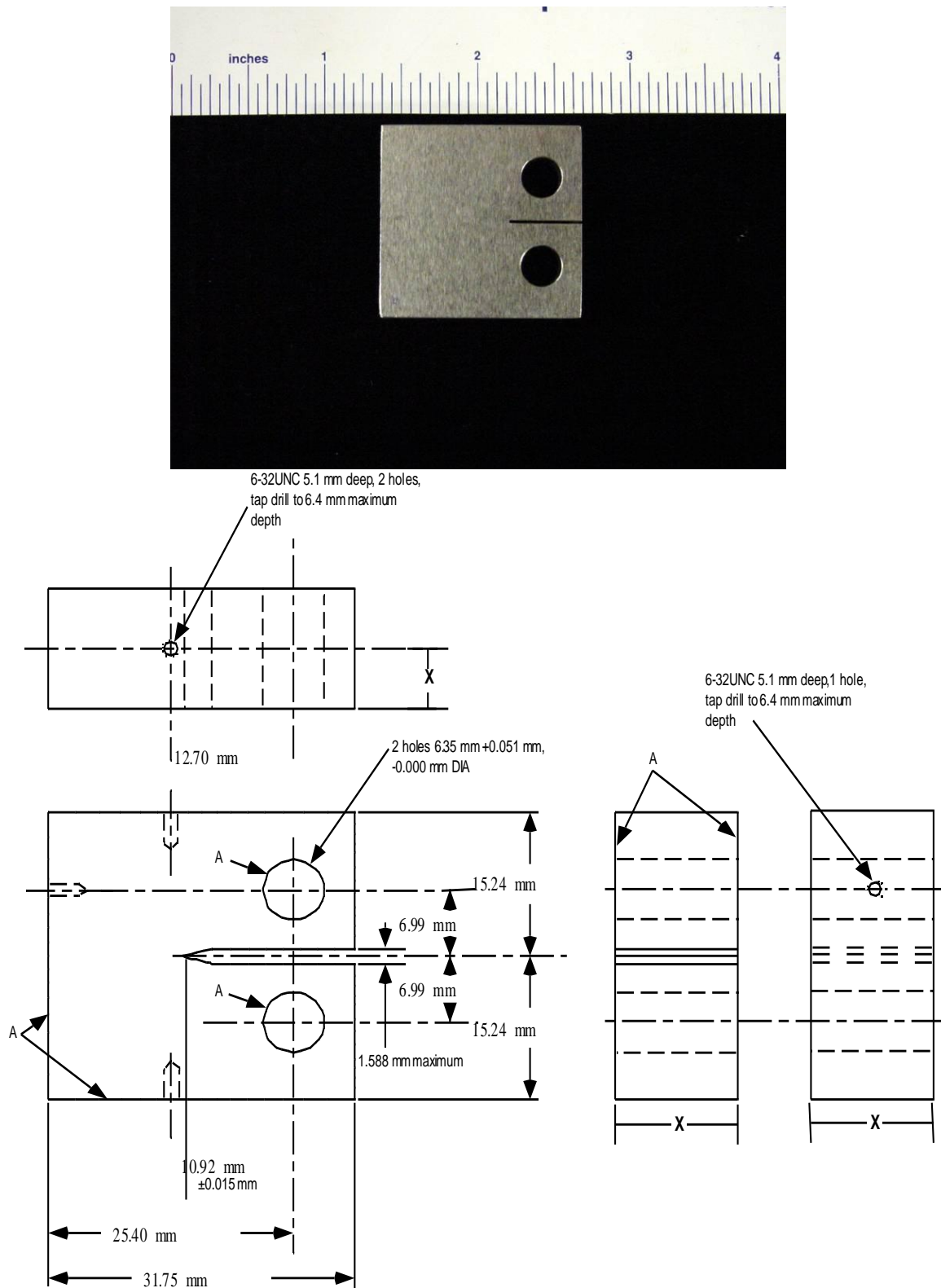


**Figure 1. Schematic of compact tension specimen.**

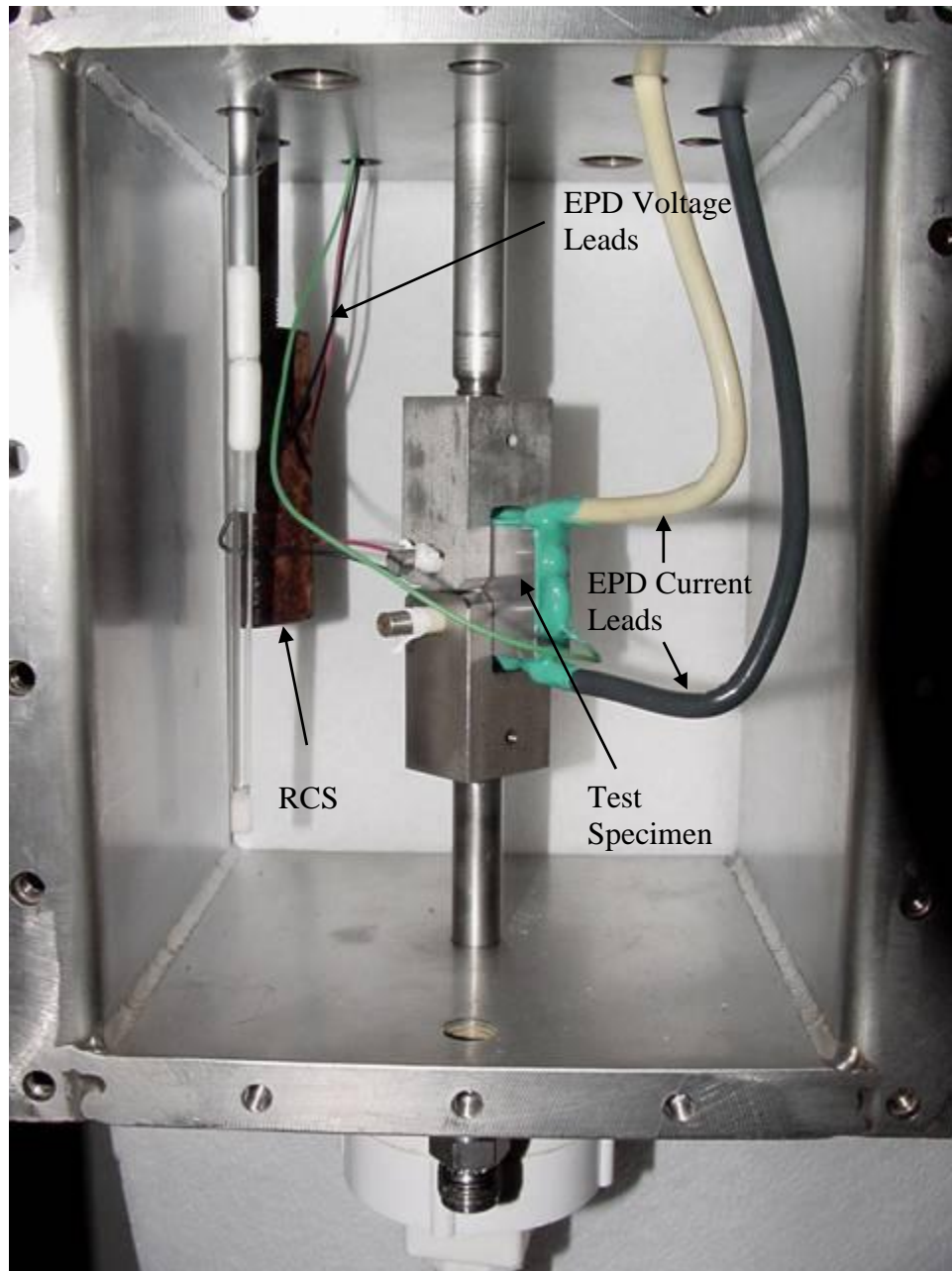


**Figure 2. Photograph of the inside of the test cell used for crack-growth testing, showing the test specimen and cell internals; RCS –Rusted Carbon Steel Sample, EPD – Electric Potential Drop.**

Flowing conditions was simulated using a jet impingement apparatus. In the jet impingement test, the flow pattern strongly depends on the ratio of the radial distance away from the jet center ( $r$ ) and the jet radius ( $r_0$ ) (Figure 3).

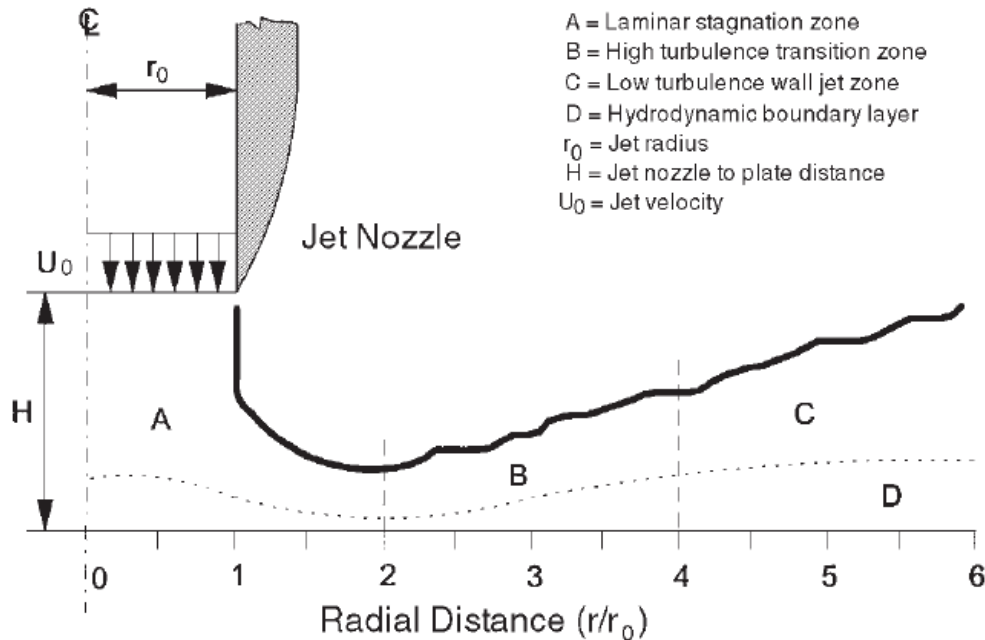


**Figure 3. Hydrodynamic characteristics of jet impingement on a flat plate showing the four characteristic flow regions \*.**

It has been demonstrated that the observed corrosion rate correlates well with that obtained under the pipe flow when the  $r/r_0$  equals three<sup>†</sup>. The wall shear stress can be calculated using the equations below<sup>‡,§</sup>:

$$\tau_w = 0.179 \rho U_0^2 \text{Re}^{-0.182} \left( \frac{r}{r_0} \right)^{-2}$$

Where:  $\tau_w$ —wall shear stress

$\rho$ —liquid density

$r$ —radial distance from the jet center

\* J.L. Dawson, C.C. Shih, "Electrochemical Testing of Flow-Accelerated Corrosion Using Jet Impingement Rigs," CORROSION/87, paper no.453 (Houston, TX: NACE, 1987).

† K. D. Eiford, E. J. Wright, J. A. Boroa, and T. G. Hailey, "Correlation of Steel Corrosion in Pipe Flow with Jet Impingement and rotating Cylinder Tests", Corrosion, v 49, N12 (1993):992

‡ F. Giralt, D. Trass, Can. J. Chem. Eng. 53 (1975): p. 505-511

§ F. Giralt, D. Trass, Can. J. Chem. Eng. 54 (1976): p. 148-155.



$r_0$ —jet radius

Re—Reynolds number defined as:

$$\text{Re} = \frac{2r_0 U_0}{\nu}$$

Where:  $U_0$ —liquid velocity

$\nu$  —liquid viscosity

Conversely, with a known target wall shear stress, one can calculate the required velocity to obtain appropriate flow pattern to simulate the pipe flow.

In the crack growth tests, the jets were positioned such that the crack tip is located in region B that typically has a high wall shear stress. Both sides of the CT sample were impinged by the flow. The testing vessel with installed jets is shown in Figure 4. The fluid jet velocity was adjusted to achieve the targeted wall shear (103 mL/min in this work).

All tests were started in the absence of inhibitors until measurable SCC crack growth has been detected. This typically took two to four weeks. The inhibitor was added to the reservoir in the flow system and the effect on crack growth was measured in-situ. If the inhibitor injected at the tested dosage is effective, the SCC crack growth rate would be expected to decrease significantly or crack growth to cease entirely.

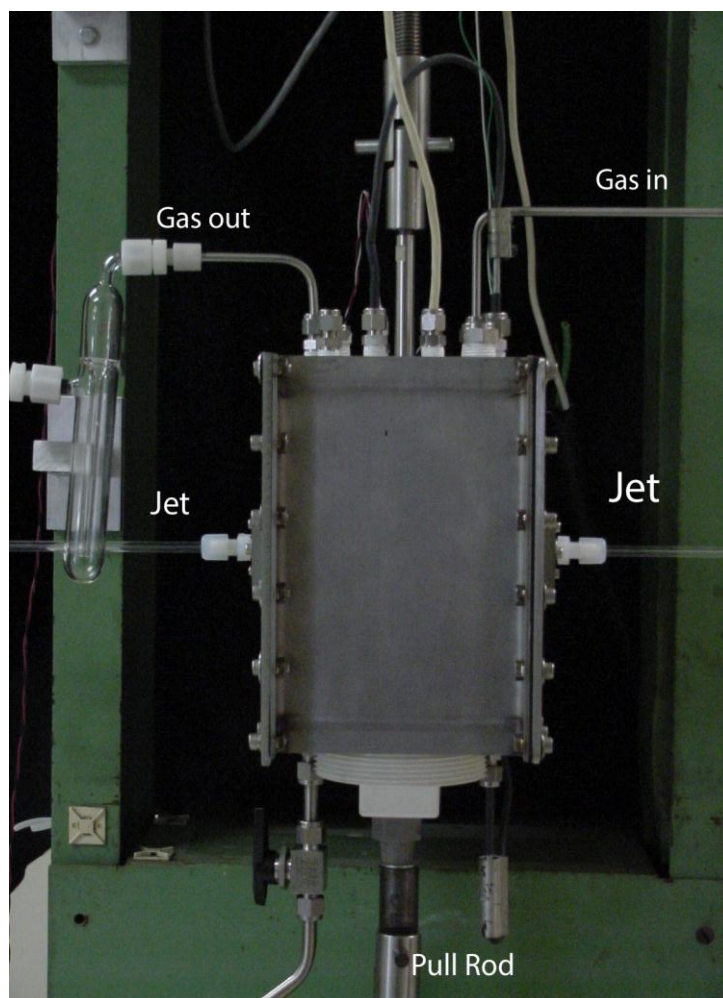


**Figure 4. Jet impingement setup to create flowing conditions on the CT sample**

### **6.3 Electrochemical Studies to Develop Rapid Selection Method for Inhibitor**

The electrochemical tests in FGE were performed using a technique developed to overcome the potential drop imposed by the resistance nature of the FGE solution<sup>\*</sup>. The polarization scans were conducted in simulated SFGE.

The samples were all 500  $\mu\text{m}$  wires (California Fine Wires<sup>†</sup>). They were prepared by mounting a wire in the epoxy (electrode surface area  $0.002\text{ cm}^2$ ). A special two parts epoxy (EPON Resin 828 and EPIKURE 3234 curing agent<sup>‡</sup>) was used owing to its extraordinary stability in organic

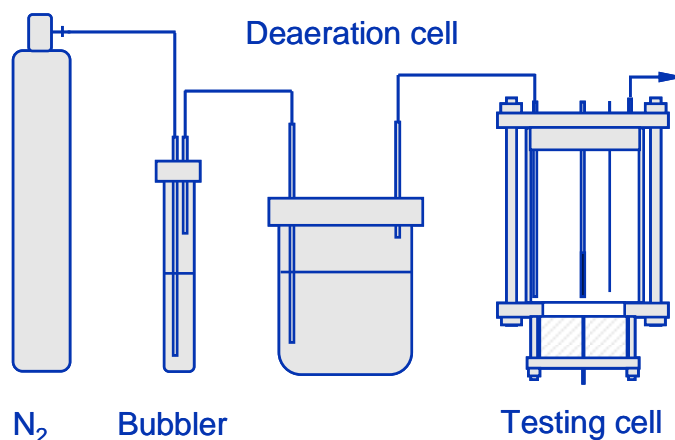
<sup>\*</sup> F. Gui and N. Sridhar, *Corrosion* 66, 4, (2010) p. 045005.

<sup>†</sup> California Fine Wire Company, Grover Beach, CA

<sup>‡</sup> Miller-Stephenson, IL, USA



solvents as demonstrated by others<sup>\*</sup>. The mounted electrodes were left in air for a few days to fully cure. They were subsequently polished with 800 grit sand paper prior to being used in the experiments. An Ag/AgCl wire was used as the reference electrode and a Pt wire was used as the counter electrode. The AgCl film on the reference electrode was prepared by galvanostatically polarizing an Ag wire in 1 M HCl for 30 mins at a current density of 0.1 mA/cm<sup>2</sup>. The reference electrode was positioned only a few millimeters away from the working electrode and the counter electrode was within 2 cm from the working electrode. The electrochemical experimental setup and the test cell used in this work are illustrated in Figure 5. Potentiodynamic polarization scans were performed on the microelectrodes using a VMP3 multichannel potentiostat (Bio-Logic)<sup>†</sup>. The open circuit potential (OCP) was monitored for one hour in each test prior to the potentiodynamic scan. The cyclic potentiodynamic polarization (CPP) scans were conducted from -100 mV vs. OCP to 0.5 V vs. Ag/AgCl at a rate of 0.17 mV/s. The scan then was reversed at 0.5 V vs. Ag/AgCl and stopped at the OCP. The cells were placed inside a faraday cage to reduce the noise during the measurement. Upon completion of the potentiodynamic scan, the working electrode was inspected under an optical microscope.

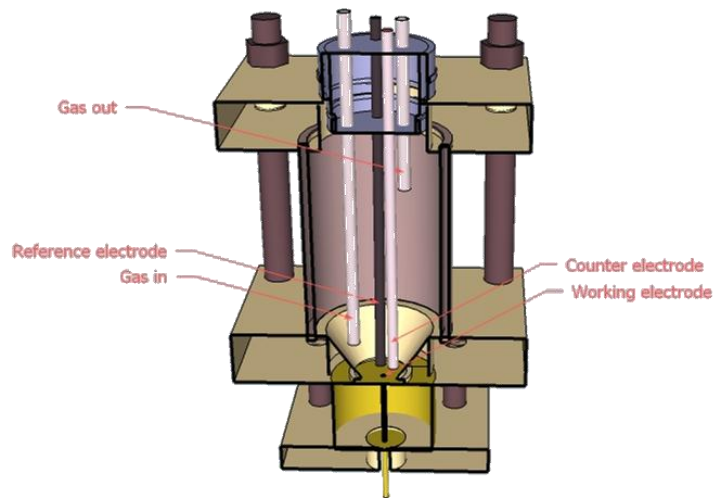


(a) experimental setup.

<sup>\*</sup> C. Amatore, M. R. Deakin and R. M. Wightman, Journal of Electroanalytical Chemistry, 225, 49(1987).

<sup>†</sup> Bio-Logic, France





(b) test cell

**Figure 5. Illustrations of the electrochemical experimental setup (a) and the test cell (b).**

SCC crack growth propagation involves environments established in occluded regions such as tight cracks. Thus, electrochemical study of the electrochemical behavior of carbon steel in occluded regions would provide insights in the crack propagation mechanism which in turn would guide the selection of effective inhibitors for SCC mitigation. Because of this, crevice corrosion study of carbon steel in SFGE was also performed.

Electrochemical tests were performed on a multielectrode array. The multielectrode array used in this work is similar to that used by Bocher et al. in their study of crevice corrosion of 316 stainless steel<sup>\*</sup>. The array consists of 100 1010 carbon steel wire (0.5 mm OD) structured as a 5 x 20 array to simulate a planar electrode (Figure 6). It was embedded in a 1" (2.54 cm) carbon steel cylinder (instead of epoxy for most multielectrode array) so that the carbon steel cylinder can serve as the external cathode to the electrodes in the array located inside the crevice. A Teflon® crevice former was assembled on the multielectrode array to form a crevice, as illustrated in Figure 7.

<sup>\*</sup> F. Bocher, F. Presuel-Moreno, N. D. Budiansky and J. R. Scully, *Electrochemical and Solid-State Letters*, 10, 3, (2007) p. C16.

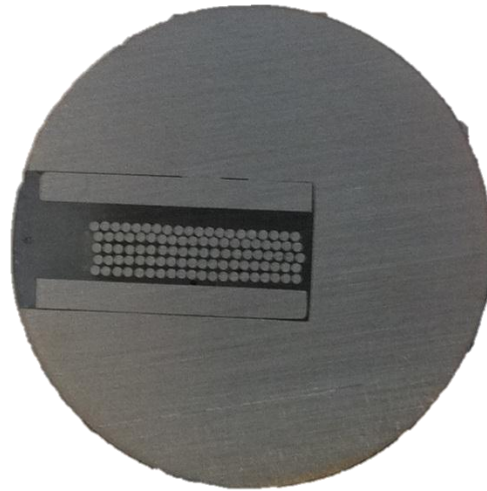


**Figure 6. Electrode array embedded in a carbon steel cylinder.**

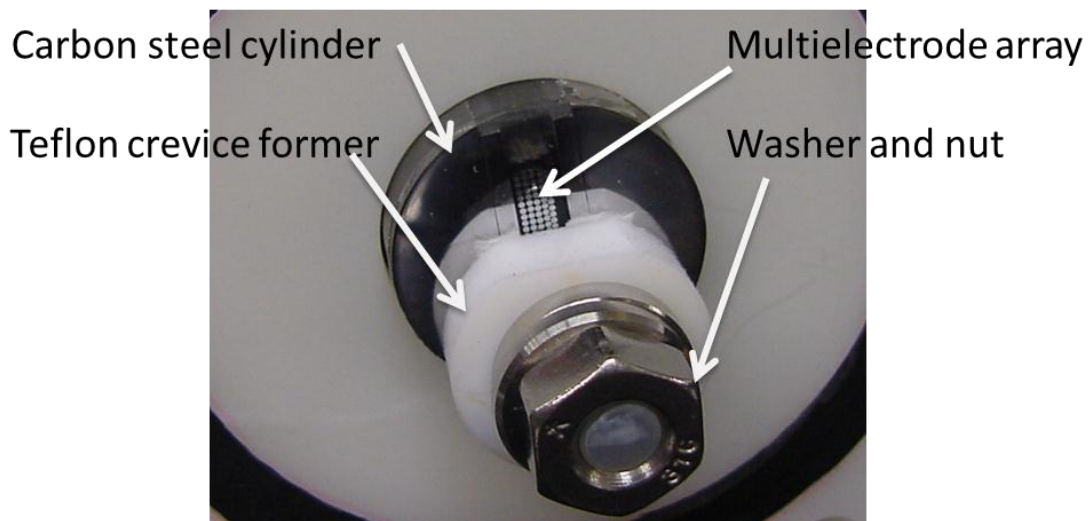


**Figure 7. Illustration of the crevice assembly.**

The multielectrode array was connected to a multichannel microelectrode analyzer (MMA)\* so that the corrosion initiation and propagation inside the crevice can be monitored over by measuring the current flowing between anodic and cathodic electrodes. All electrochemical tests were performed under open circuit potential (OCP). For tests performed under deaerated conditions, the solution was purged with nitrogen over night to make sure oxygen was fully removed. The solution was then transferred to the testing cell using nitrogen to avoid oxygen contamination. Tests under aerated conditions were performed in SFGE purged either by

\* Scribner Associates, Southern Pines, NC 28387

compressed air or 1% (volume) oxygen balanced with nitrogen. At the end of each test, the electrode array was inspected under a stereomicroscope to confirm the attack (or the lack thereof). The current measured on each electrode was integrated over the testing time to obtain the charge. The latter was then converted to the depth of attack that was used to quantify the corrosion extent inside the crevice in different conditions.

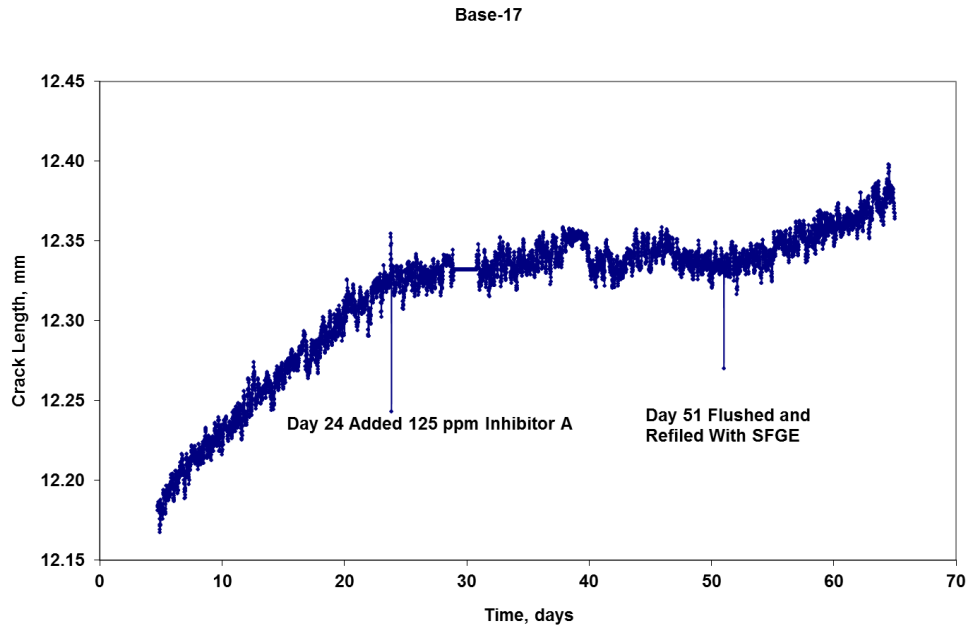
## 7.0 RESULTS

### 7.1 Task 1: Inhibitor Performance Evaluation

#### 7.1.1 Inhibitor performance under flowing conditions

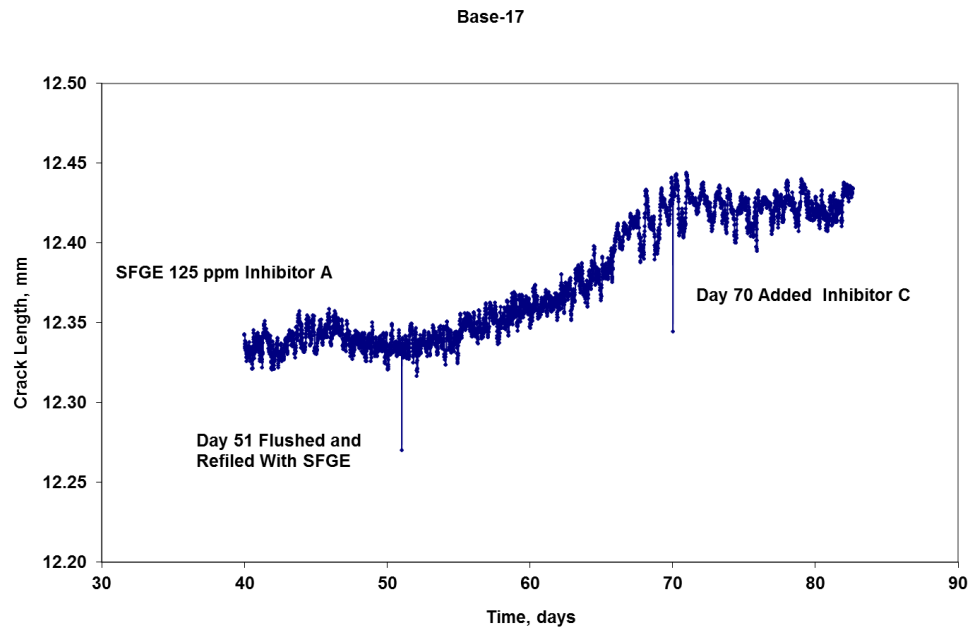
To evaluate the performance under flowing conditions, the sample was exposed to SFGE with the crack tip located in turbulent region of the impinged flow. The test was performed to establish stable crack growth prior to introducing the inhibitor. As mentioned before, an effective inhibitor typically would result in the change in the slope of the crack length vs. time. The crack length changes as a function of time for each step during the test (SFGE/FGE with and without inhibition addition) are shown from Figure 8 to Figure 11. The crack growth rate during each step can be found in the Appendix for specimen Base-17.

Figure 8 shows the crack length vs. time for the specimen used in the jet impingement test to evaluate Inhibitor A. As shown, prior to the injection of the inhibitor on Day 24, stable crack growth was established. The crack was stalled after the addition of 125 ppm Inhibitor A from Day 24 to Day 51 showing a nearly zero slope. This indicates the Inhibitor A was able to mitigate the growing crack even under turbulent flowing condition created by the jet impingement apparatus.

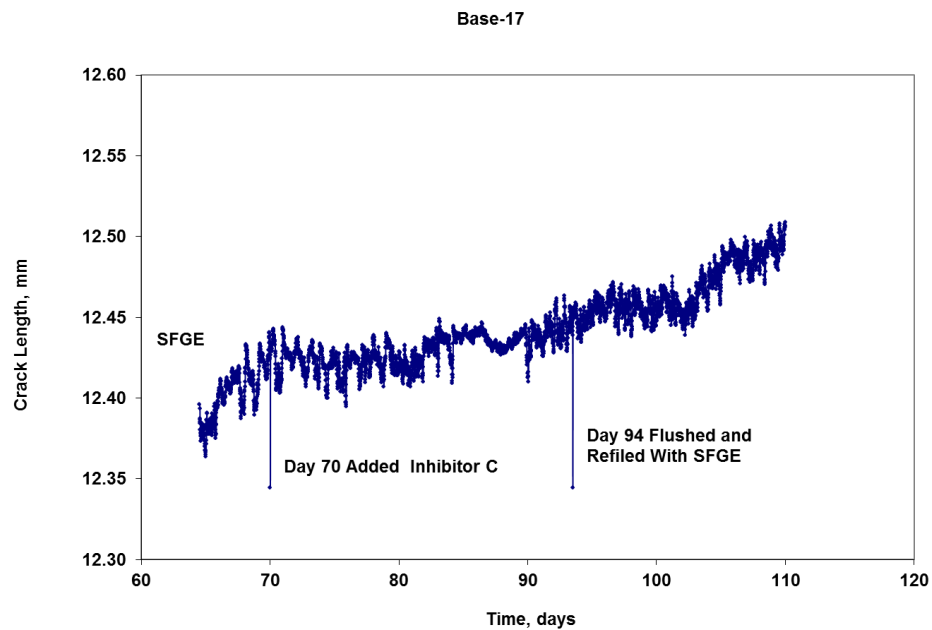


**Figure 8. Crack length as a function of time for Base-17 under flowing SFGE to evaluate Inhibitor A.**

On Day 51, the solution was replaced with fresh prepared SFGE so that crack can propagate again. This is shown in Figure 9 (a). Stable crack growth was re-established from Day 51 and Day 70. The Inhibitor C was added on Day 70 after the stable crack has propagated for 20 days. The slope of the curve clearly changed from Day 70 after the addition of the inhibitor to a nearly zero value, indicating the Inhibitor C was efficient in mitigating SCC under turbulent flowing condition (see also Figure 9 (b)).



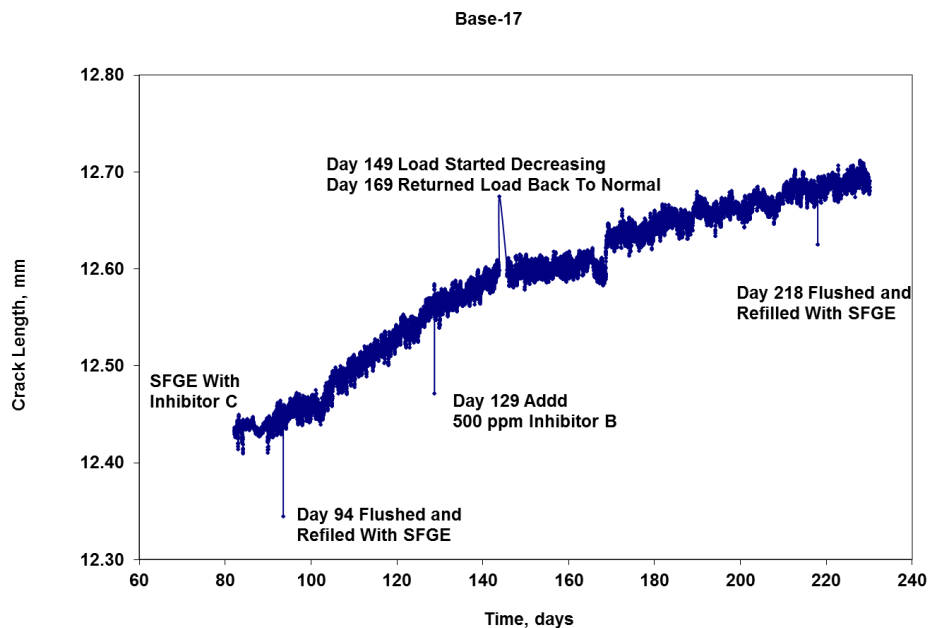
(a)



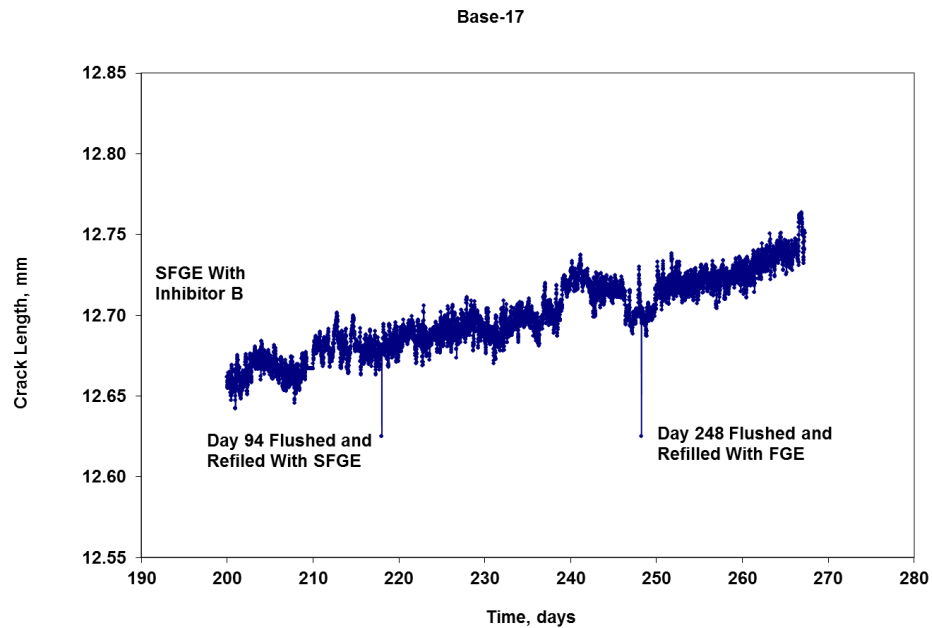
(b)

Figure 9. Crack length as a function of time for Base-17 under flowing SFGE to evaluate Inhibitor C.

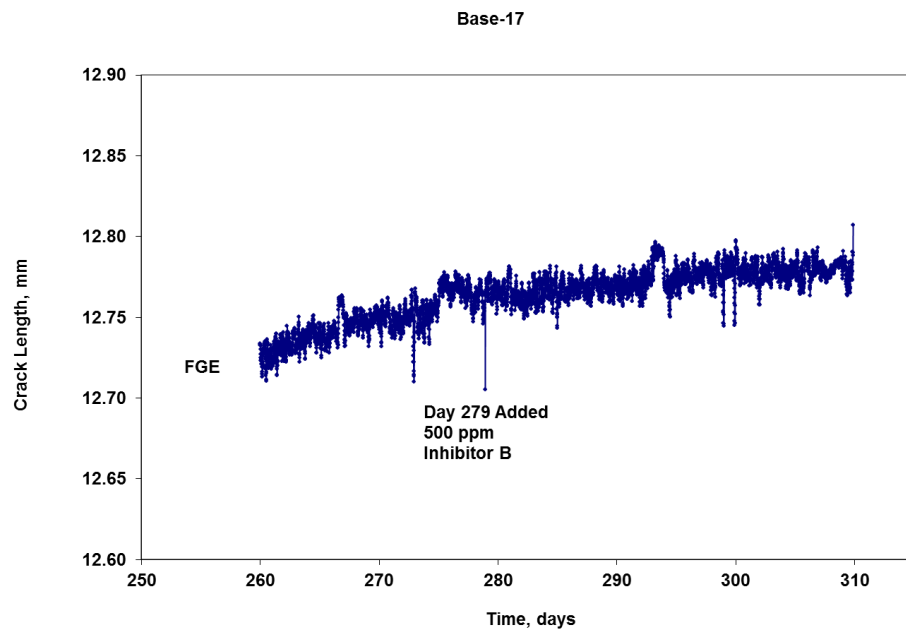
The test was continued with the same procedure (i.e., establish stable crack growth→inject inhibitor→flush solution to re-establish crack growth) to evaluate INHIBITOR B in SFGE (Figure 10) and in FGE (Figure 11). The mitigation of SCC by INHIBITOR B can be seen in Figure 10 from Day 129 to Day 169. The INHIBITOR B did not appear to be function to stall the crack growth immediately after injection as observed for others above. Rather, it took about 20 days for the slope of the curve to change to a near plateau. During this testing duration, the load on the sample changed slightly and it is uncertain whether this contribution to above observation. Because of this, INHIBITOR B was tested again but in FGE. As shown in Figure 11, the solution was replaced with a FGE lot that was supplied by ADM on Day 248. Stable crack was noted from Day 248 to Day 279 in the FGE. INHIBITOR B was added on Day 279 and the slope of the crack length vs. time started to change after the addition of the inhibitor (Figure 11 (b)). The test is still running to get more data points to show a clearer trend in the plateau and the results will be updated in the final version of the report.



**Figure 10. Crack length as a function of time for Base-17 under flowing SFGE to evaluate INHIBITOR B.**



(a)



(b)

**Figure 11. Crack length as a function of time for Base-17 under flowing FGE to evaluate INHIBITOR B.**

### 7.1.2 Threshold concentration evaluation

The inhibitors selected to be used in this work were demonstrated in the PRCI SCC 4-3 Phase II project using either slow strain rate (SSR) test or crack growth rate test. However, no efforts were taken in the PRCI project to evaluate these inhibitors would still provide efficient SCC mitigation at a concentration lower than the standard dosage shown in Table 2. Lower concentration in many cases would be benefit with respect to operation cost reduction or meeting the fuel standard (e.g., in the case of  $\text{NH}_4\text{OH}$  since  $\text{NH}_4\text{OH}$  addition tends to increase the solution pH). This section summarizes the results of the tests performed to evaluate these selected inhibitors focusing on the performance evaluation at concentrations lower than the recommended dosage.

Figure 12 shows the crack length as a function of time for sample Base-10 used to evaluate the threshold concentration of Inhibitor A. As shown, 125 ppm of Inhibitor A was added on Day 834 after stable crack growth was established from Day 780 to Day 834. The crack continues to growth without showing any changes in the slope of the curve. This suggests that the inhibitor was not effective in mitigate SCC at half of the standard concentration. No further efforts were taken to evaluate the concentration levels between 125 ppm and 250 ppm.

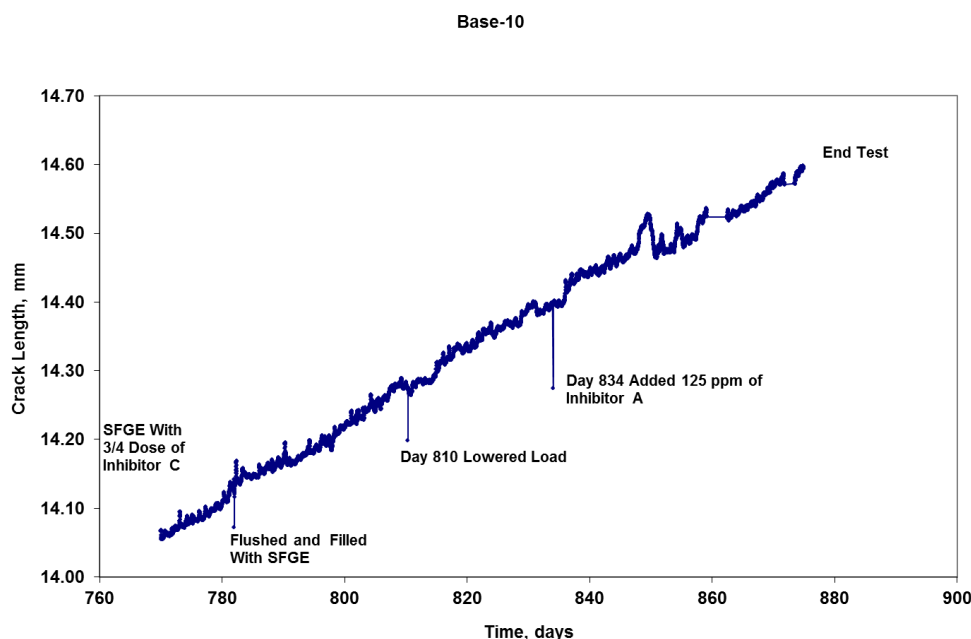


**Figure 12. Crack length change as a function of time for sample Base-9 to evaluate the threshold concentration of Inhibitor A in SFGE.**

Similar performance evaluation was performed form Inhibitor C, as shown in **Figure 13**. Half dose was added on Day 597 when stable crack growth was established. No changes were observed on the slope of the curve. Another  $\frac{1}{4}$  dose of the inhibitor was added again on Day 643 so the concentration of the inhibitor in the solution was  $\frac{3}{4}$  of the standard concentration. The



crack still kept propagation suggesting the inhibitor was not effective at concentration levels lower than the recommended dosage.

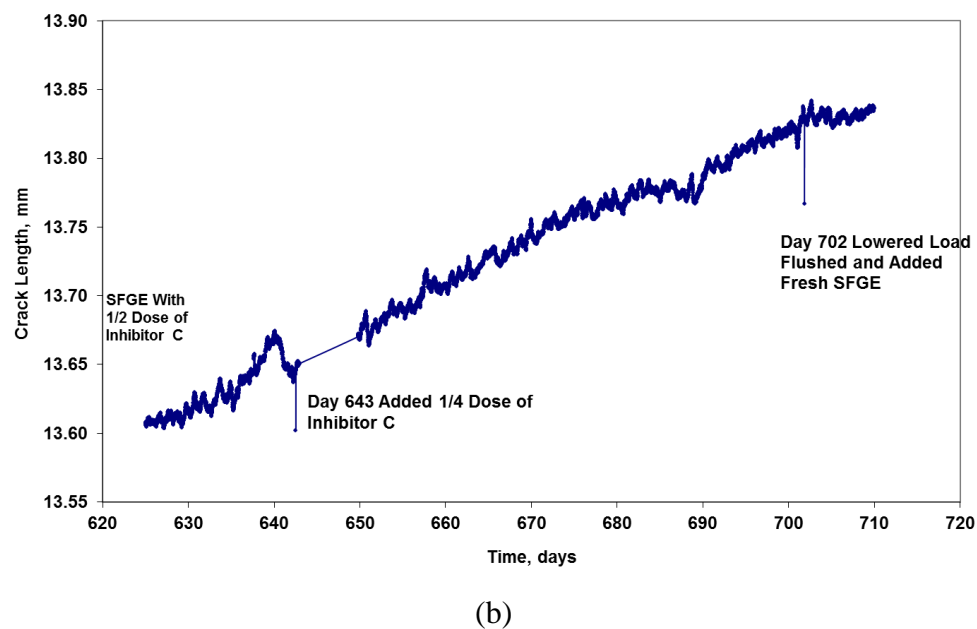
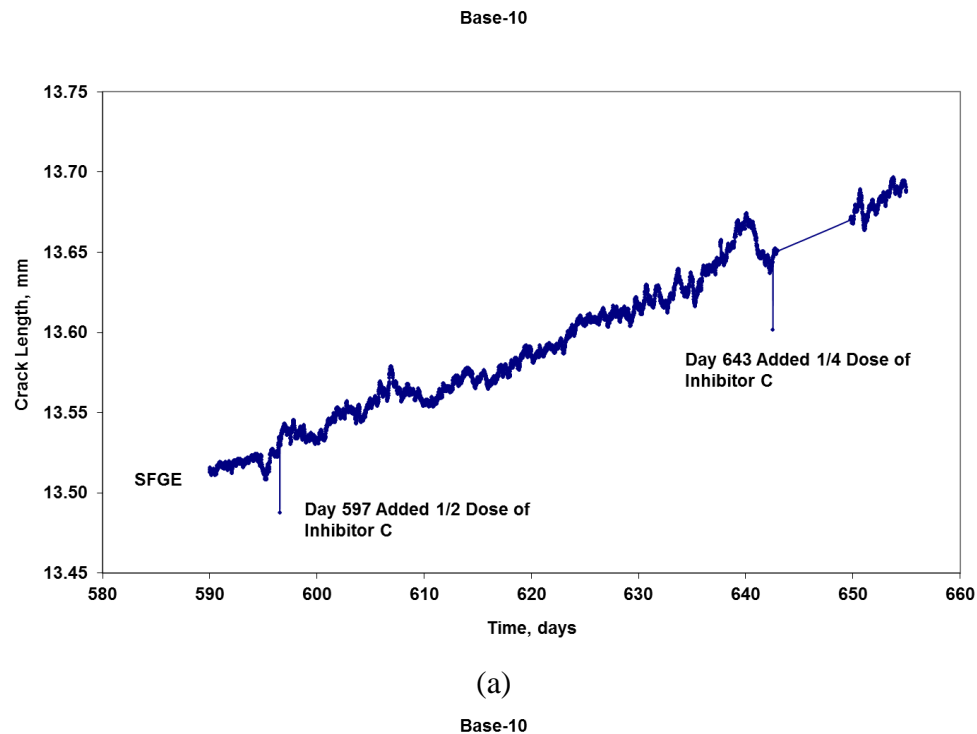


**Figure 13. Crack length change as a function of time for sample Base-10 to evaluate the threshold concentration of Inhibitor C.**

Figure 14 shows the evaluation of the threshold concentration of INHIBITOR B. Half dosage was added on Day 321 when stable crack propagation was observed on the sample. The slope of the curve changed dramatically soon after the addition of the inhibitor to a nearly horizontal one, indicating a minimal crack growth rate. This suggest that the INHIBITOR B was still effective at half dosage (250 ppm) in mitigate carbon steel SCC in SFGE.

HAZ-2

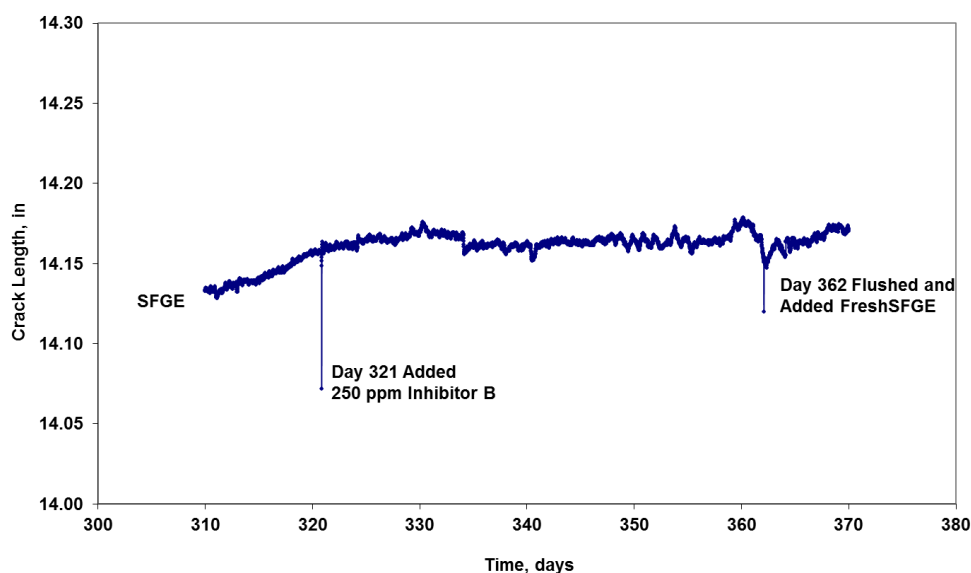


**Figure 14. Crack length change as a function of time for sample Base-11 to evaluate the threshold concentration of INHIBITOR B in SFGE.**

It has been shown previously in the PRCI and PHMSA funded projects that  $\text{NH}_4\text{OH}$  is very effective in mitigating carbon steel SCC in SFGE/FGE at small concentrations. The addition of  $\text{NH}_4\text{OH}$ , however, will increase the pHe of the FGE solution. As shown in Table 3, the pHe of the FGE solution increased to above near or above 9 when 75 ppm  $\text{NH}_4\text{OH}$  was added. When 37.5 ppm of  $\text{NH}_4\text{OH}$  was added, the pHe of the FGE solution reached near 9. Note that the current ASTM fuel standard requires the pHe of the fuel to be between 6 and 9. These two concentration levels have been demonstrated to be very effective to mitigate SCC. Thus, it is essential to evaluate whether SCC in FGE can be mitigated at a concentration lower than 37.5 ppm.

**Table 3. Solution pHe change with different concentrations of  $\text{NH}_4\text{OH}$ .**

Concentration $\text{NH}_4\text{OH}$	FGE		SFGE
	#1602553	#1527139	
0 ppm	7.07	7.24	5.23
18.75 ppm	8.36	8.78	
37.50 ppm	8.67	8.97	
75.00 ppm	8.99	9.38	

Figure 15 shows the crack length as a function of time in the evaluation of the  $\text{NH}_4\text{OH}$  performance at 18.75 ppm. The inhibitor was added on Day 725 after establishing stable crack propagation from Day 702 to Day 725. The crack kept propagating after the addition of the inhibitor for approximately two months until the solution was flushed on Day 782. The results suggest that  $\text{NH}_4\text{OH}$  was not effective at 18.75 ppm in mitigate SCC.

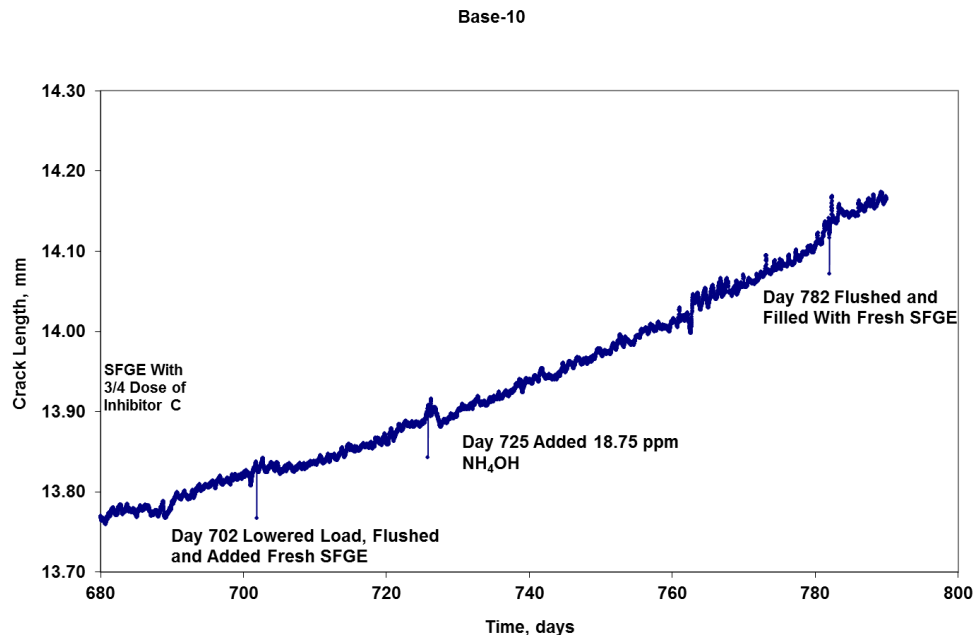
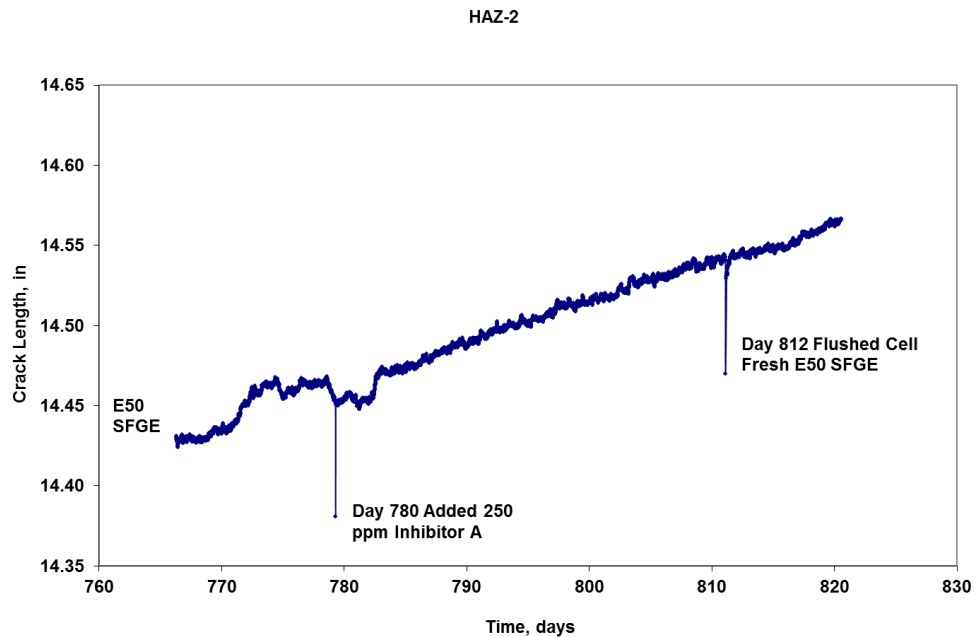


**Figure 15. Crack length change as a function of time for sample Base-10 to evaluate the threshold concentration of  $\text{NH}_4\text{OH}$  in SFGE.**

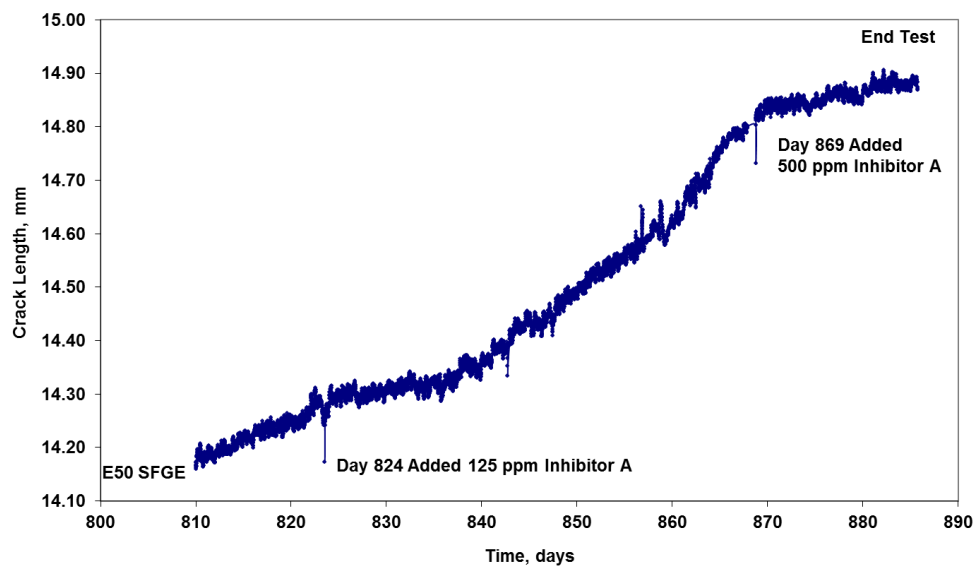
SCC was found to be more severe in E50 than in E95 in PHMSA funded project (#WP325). This work investigated whether the inhibitors demonstrated effective in E95 would be still effective in E50. The results are summarized from Figure 16 to Figure 17.

Figure 16 shows the crack length as a function of time for sample HAZ-2 used to evaluate Inhibitor A in E50. As shown, 250 ppm of the inhibitor was added on Day 780 after establishing stable crack growth in E50. No changes were seen on the slope of the curve indicating the inhibitor was not effective at 250 ppm to mitigate SCC in E50. The solution was replaced with fresh E50 on Day 812 and 125 ppm of the inhibitor was added on Day 824. Half concentration was added since the solution was fresh and this concentration level in E50 was not evaluated before. The crack did not stall with 125 ppm Inhibitor A. Another 500 ppm of the same inhibitor was then added on Day 869 and the slope of the curve changed soon after the addition showing a lower crack growth rate. The results seem to suggest that the concentration that is needed to mitigate SCC in E50 could be higher than in E95. In the case of Inhibitor A, the effective concentration level in E50 was 625 ppm whereas it was 250 ppm in E95.



(a)

Base-9



(b)

**Figure 16. Crack length change as a function of time for samples HAZ-2 and Base-9 to evaluate the threshold concentration of Inhibitor A in E50.**

Similar performance evaluation in E50 was conducted for INHIBITOR B and  $\text{NH}_4\text{OH}$ , as shown in Figure 17 and Figure 18, respectively. As shown in Figure 17, INHIBITOR B was able to stall

the crack growth at a concentration of 3000 ppm. Note this concentration is much higher than the standard concentration and was used because the crack growth rate was significantly fast so that the remaining ligament on the sample was approaching the maximum useful range. In order to be able to still use the sample, a high dosage of the inhibitor was used to be able to stall the crack growth rapidly. No lower concentration of INHIBITOR B than this level was evaluated in E50.

Base-15

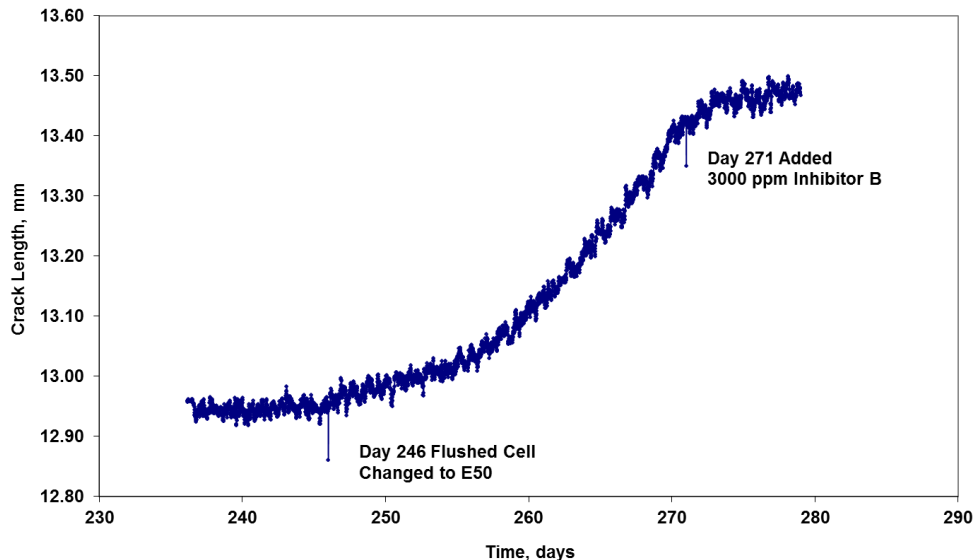


**Figure 17. Crack length change as a function of time for sample Base-15 to evaluate the threshold concentration of INHIBITOR B in E50.**

NH<sub>4</sub>OH at 37.5 ppm was still able to stall the propagating crack in E50, as shown in Figure 18. The pHe of E50 is typically ~6 so adding 37.5 ppm NH<sub>4</sub>OH will unlikely increase the pHe to a level higher than the ASTM specification of 9. Therefore, it appears to be feasible to use NH<sub>4</sub>OH at 37.5 ppm in E50 to mitigate carbon steel SCC.

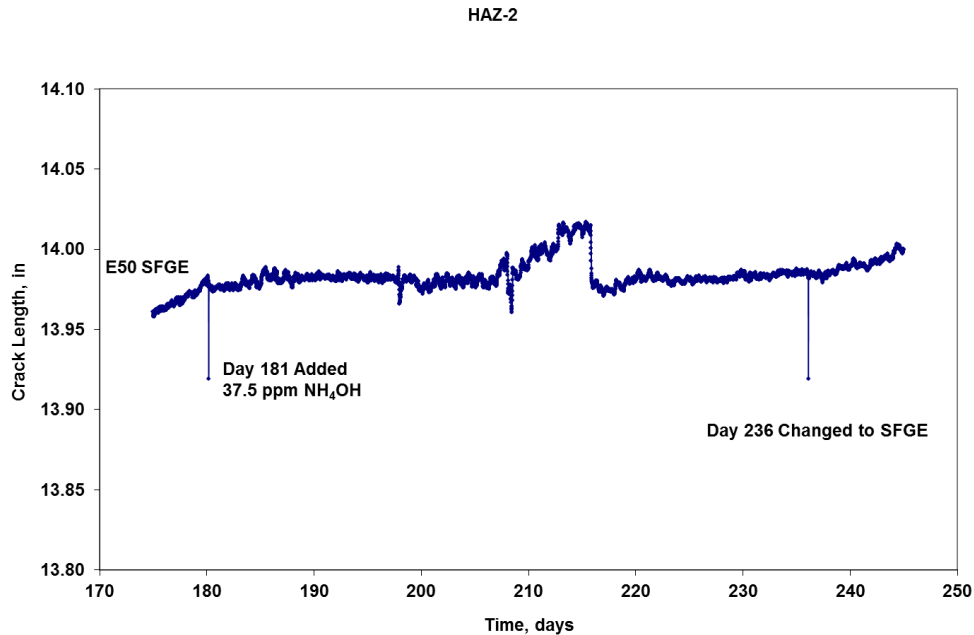
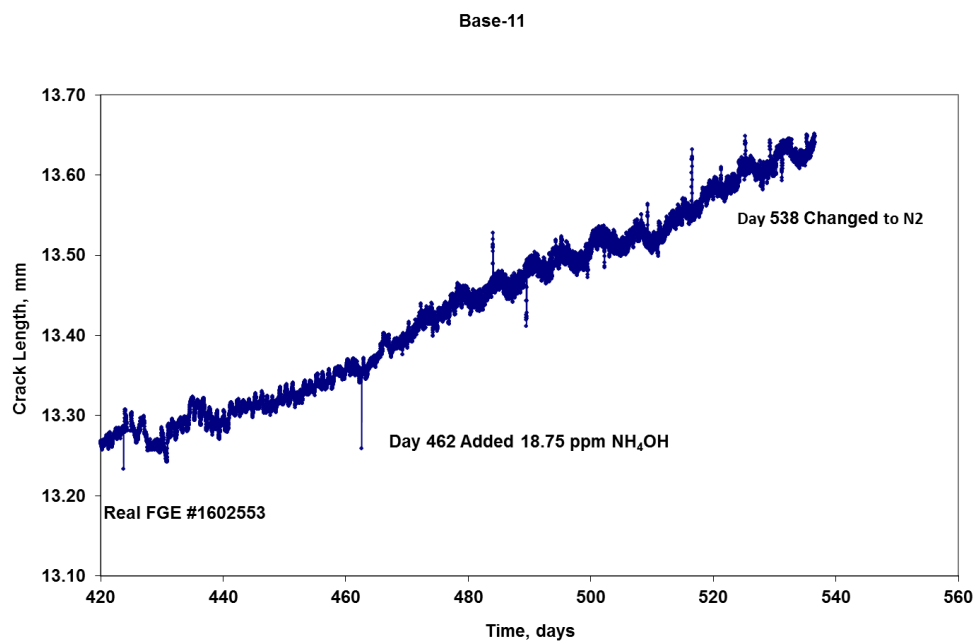


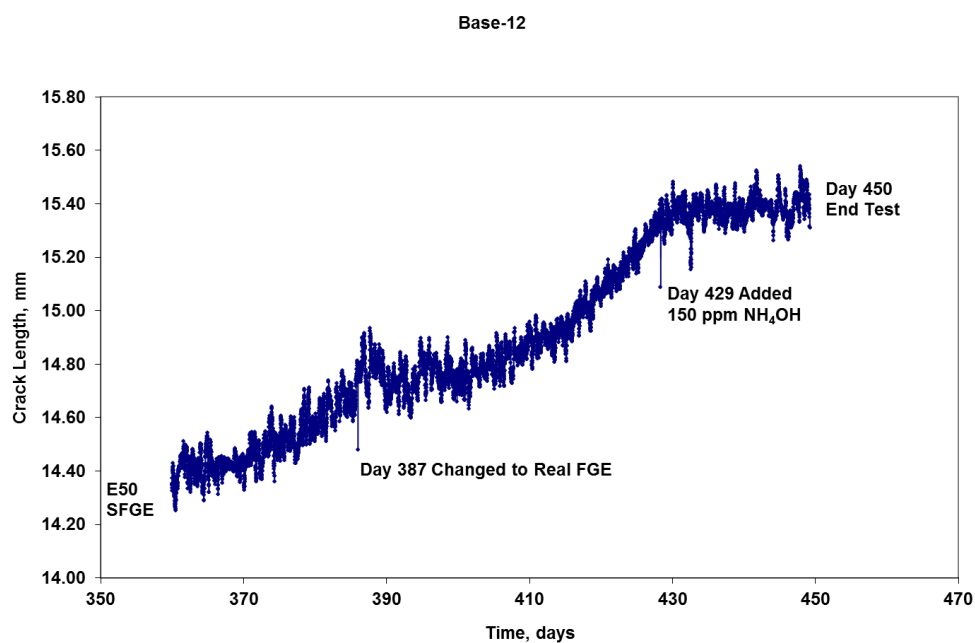
**Figure 18. Crack length change as a function of time for sample HAZ-2 to evaluate the threshold concentration of  $\text{NH}_4\text{OH}$  in E50.**

Most of the work performed in previously completed projects on inhibitor performance focused on their performances in SFGE. It has been shown in the previous section that INHIBITOR B was effective under flowing conditions to mitigate SCC in FGE. Some tests were performed in this work on selected inhibitors with respect to their performance in FGE at concentrations lower than the standard level.

Figure 19 shows the crack length as a function of time for sample Base-11 and Base-12 evaluating  $\text{NH}_4\text{OH}$  performance in FGE. As shown,  $\text{NH}_4\text{OH}$  was not able to mitigate crack growth at 18.75 ppm (Figure 19 (a)) but was effective at 150 ppm (Figure 19 (b)). The high concentration was used when the sample remaining ligament was approaching the maximum useful limit to see inhibitor effect rapidly. Previous tests have demonstrated that 37.5 ppm  $\text{NH}_4\text{OH}$  was an effective concentration to stall the crack growth in both FGE and SFGE.



(a)



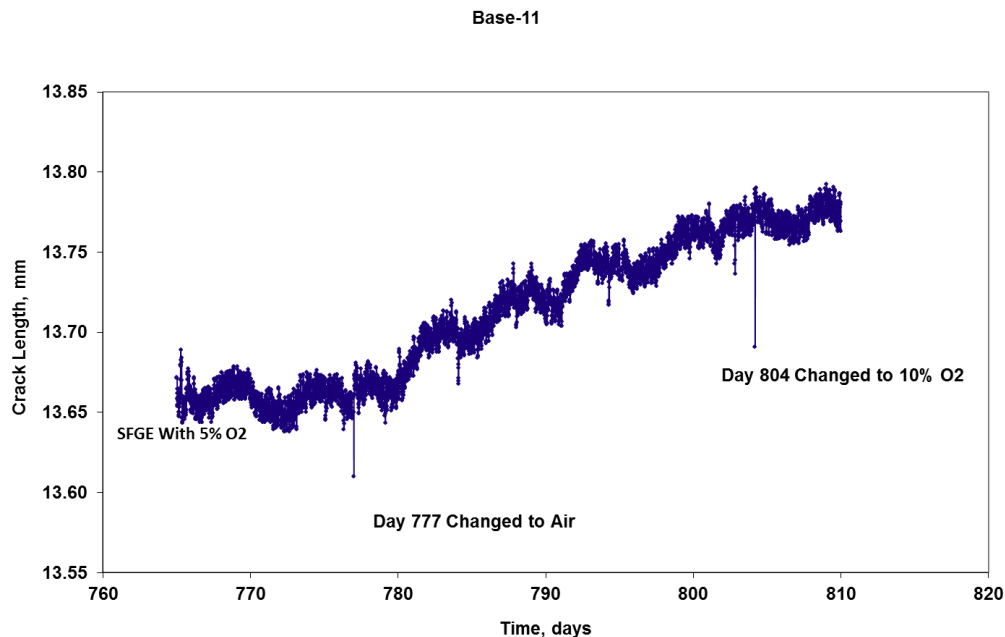
(b)

**Figure 19. Crack length change as a function of time for samples Base-11 and Base-12 to evaluate the threshold concentration of  $\text{NH}_4\text{OH}$  in FGE.**

### 7.1.3 Threshold oxygen concentration evaluation

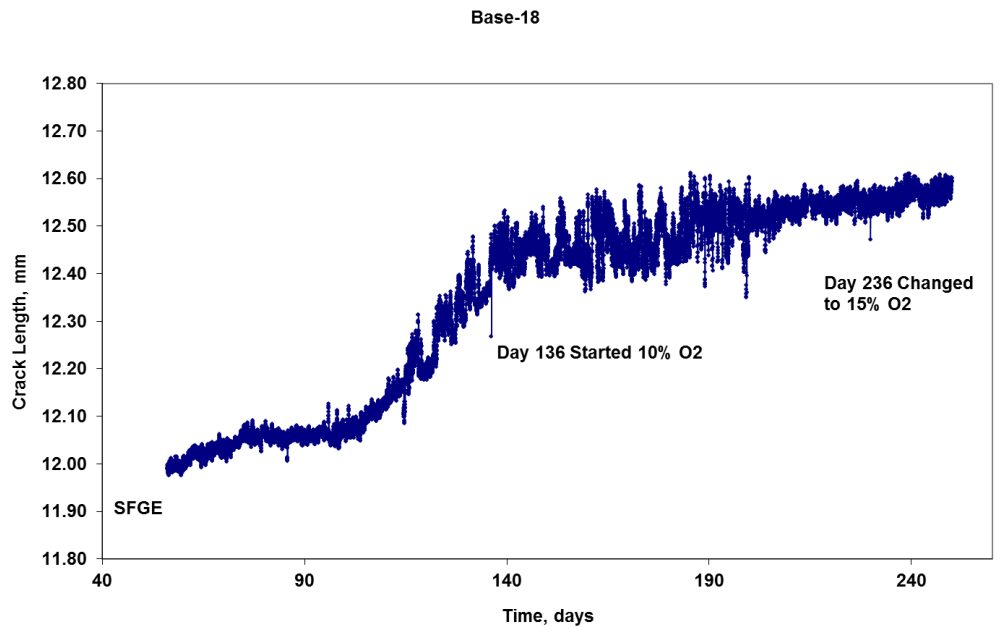
It has been reported before that the threshold concentration of oxygen for SCC in FGE is approximately 1% in the gas phase. This corresponds to ~4 ppm of dissolved oxygen. This result, however, was based on SSR tests that tend to be more aggressive than other techniques, especially for mild cracking environment such as FGE. Thus, the threshold oxygen concentration was investigated in this work using CT samples.

Figure 20 shows the crack length as a function of time for sample Base-11 that evaluated the threshold oxygen concentration for SCC. As shown, the cured exhibited a nearly horizontal slope when the solution was purged with 5% oxygen prior to Day 777, indicating stable crack propagation was not possible in when the gas phase contains 5% oxygen. Stable crack propagation was established by purging the solution with air from Day 777 to Day 804. The gas then was switched to 10% oxygen with the slope changed after the introduction of 10% oxygen. Based on these results, the threshold oxygen concentration would be higher than 10%. This was confirmed with sample Base-18. As shown in Figure 21, the crack stalled again with 10% oxygen purging but was able to propagate with 15% purging. This observation suggests that the threshold oxygen concentration for SCC is between 10% and 15%, corresponding to a dissolved oxygen concentration of ~40 ppm and ~60 ppm, respectively.

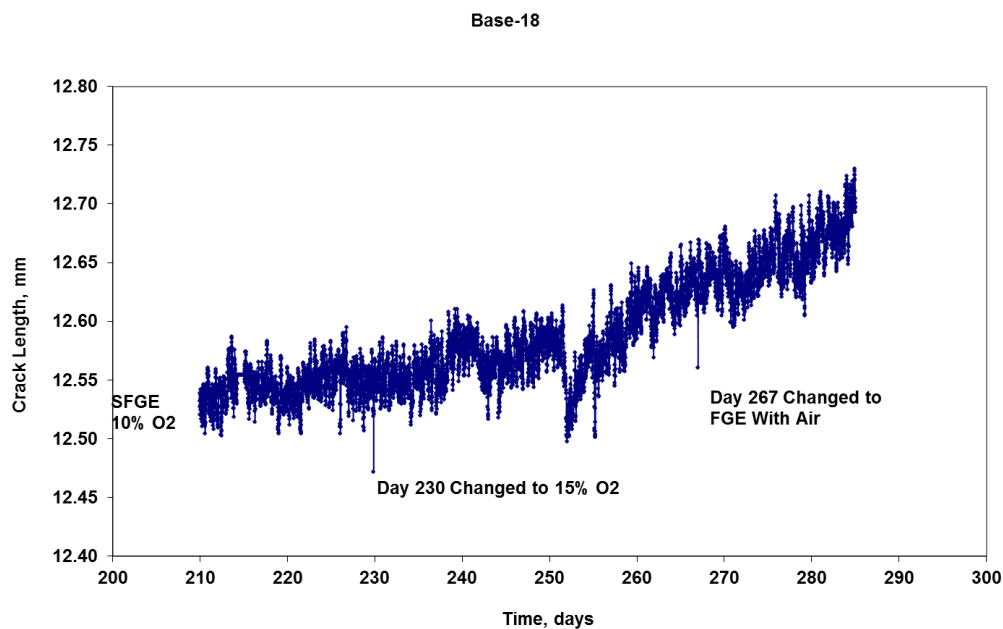


**Figure 20. Crack length as a function of time for Base-11 sample to evaluate the threshold oxygen concentration for cracking.**





(a)



(b)

**Figure 21. Crack length as a function of time for Base-18 sample to evaluate the threshold oxygen concentration for cracking.**

## 7.2 Task 2: Rapid Inhibitor Selection Method

### 7.2.1 Electrochemical behavior of carbon steel in inhibited SFGE

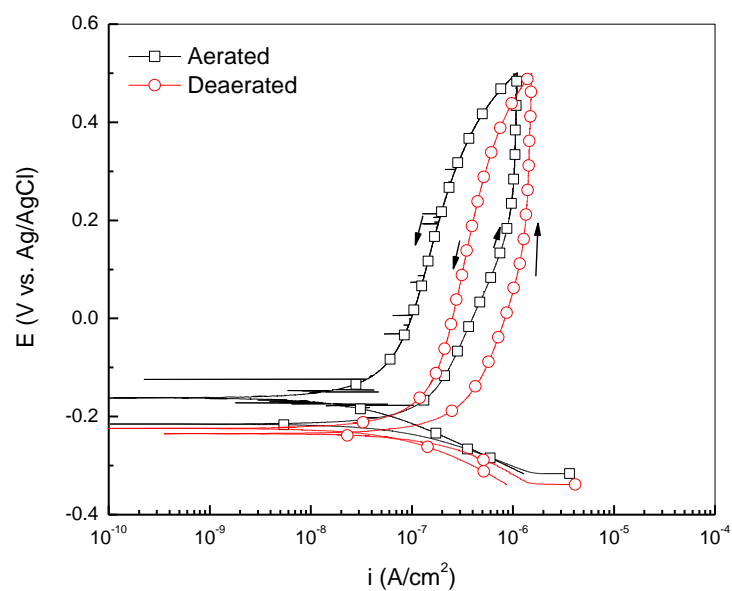
Although inhibitor performance can be evaluated by performing SSR test or crack growth rate tests to select the proper one for a specific application, these techniques can be time and cost consuming. A simpler and easier technique is desired to select inhibitor especially in the initial screening phase. In this regard, electrochemical test is a good technique that could assist in the selection of inhibitors for carbon steel SCC in FGE.

Figure 22 shows the comparison of the polarization curves performed in SFGE containing two inhibitors under deaerated and aerated conditions. As shown, the difference between Figure 22 (a) and (b) is that the polarization curve obtained in deaerated condition. For the inhibitor in (a), the curves were almost identical in deaerated and aerated condition with the specimen shown no corrosion attack after testing. For the inhibitor in (b), however, the curve obtained in deaerated solution showed an open loop with the sample shown corrosion attack after testing. From CGR testing, it was found that inhibitor in Figure 22 (a) could in fact stall the crack growth while the inhibitor used in Figure 22 (b) was not effective, as shown in Figure 23.

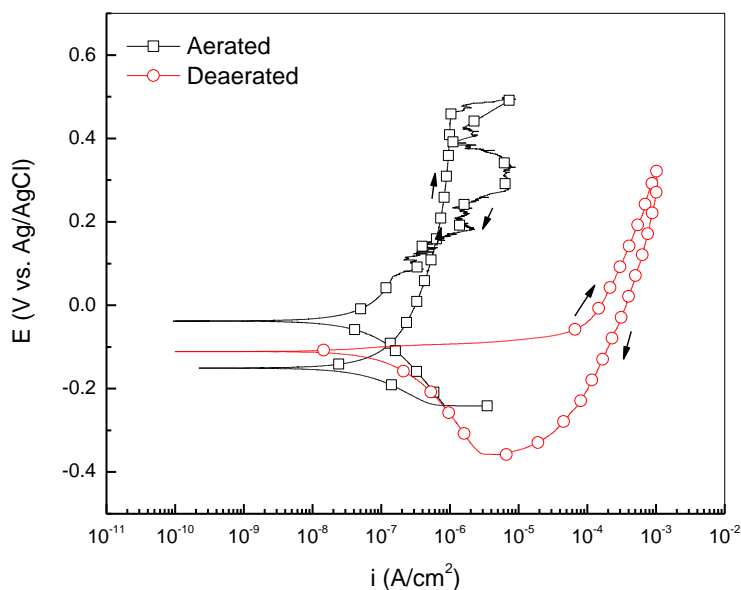
These results seem to imply that an inhibitor that works in mitigating corrosion in deaerated FGE would also be able to have the potential as a SCC inhibitor. This observation is consistent with the mechanistic study performed before. It has been demonstrated that carbon steel can experience more severe attack under deaerated SFGE than in aerated solution due to the lack of passivity when oxygen is absent in deaerated conditions<sup>\*</sup>. A possible role of oxygen in promoting carbon steel SCC in FGE is its ability to protect the crack wall while polarizing the crack tip which might be under deaerated condition or lack of passive film on the fresh exposed metal from plastic straining<sup>†</sup>. Thus, it would make sense for an inhibitor to be able to stop the corrosion at the crack tip (under deaerated condition or lack of passive film) in order to stall the crack propagation.

<sup>\*</sup> F. Gui, N. Sridhar and J. A. Beavers, *Corrosion*, 66, 12, (2010) p. 125001

<sup>†</sup> F. Gui, N. Sridhar and J. A. Beavers, *Corrosion*, 66, 12, (2010) p. 125001

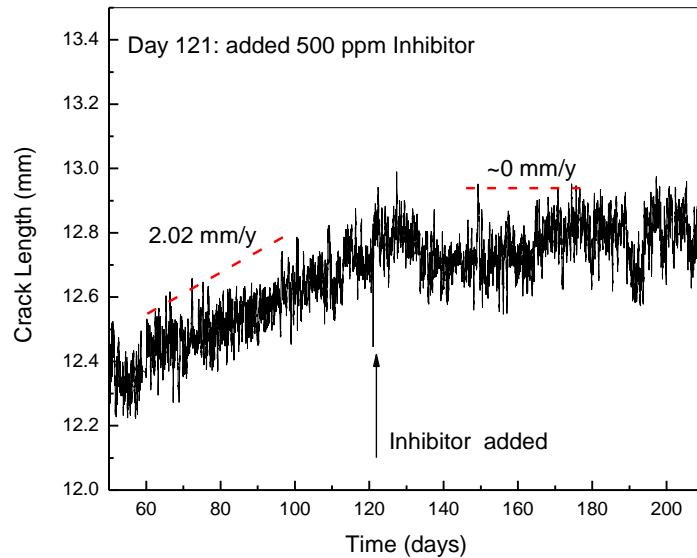


(a)

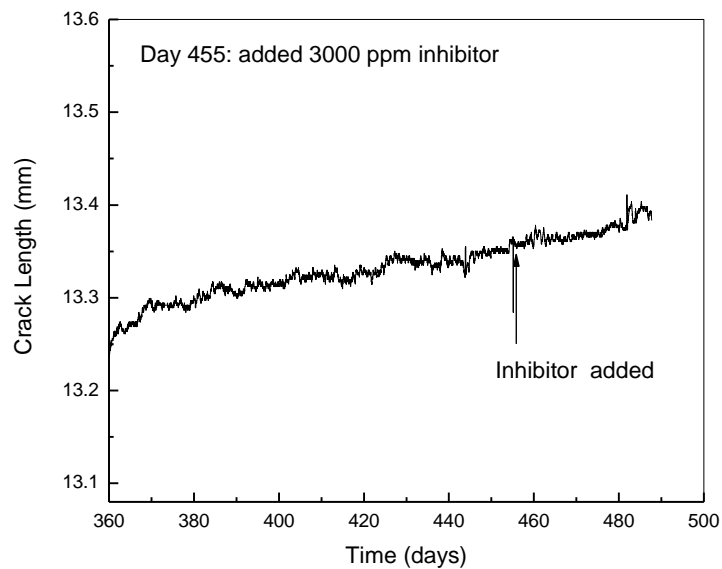


(b)

**Figure 22: Comparison of polarization curves of carbon steel in SFGE containing an inhibitor that was effective in mitigating SCC (a) and an inhibitor that was not effective in mitigating SCC (b).**



(a) performance of the inhibitor used in Figure 22 (a)



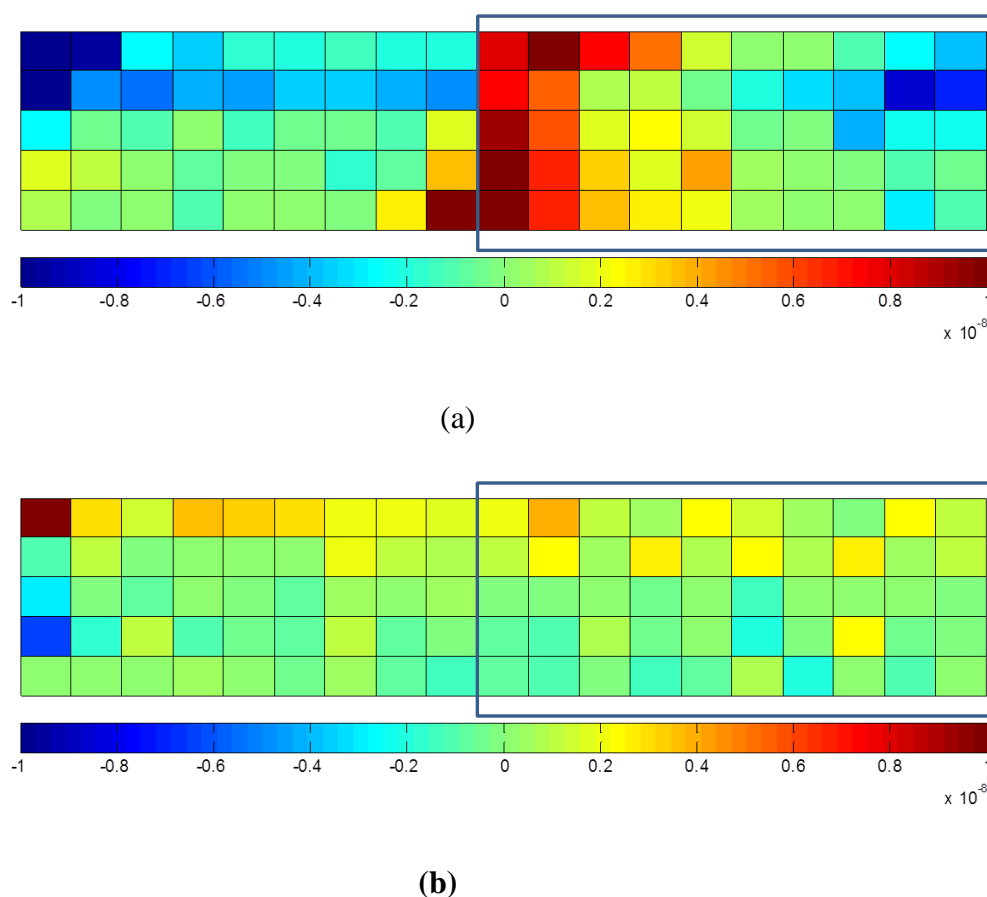
(b) performance of the inhibitor used in Figure 22 (b)

**Figure 23: Crack length and growth rate as a function of time before and after inhibitors were injected.**

### 7.2.2 Crevice corrosion of carbon steel in SFGE

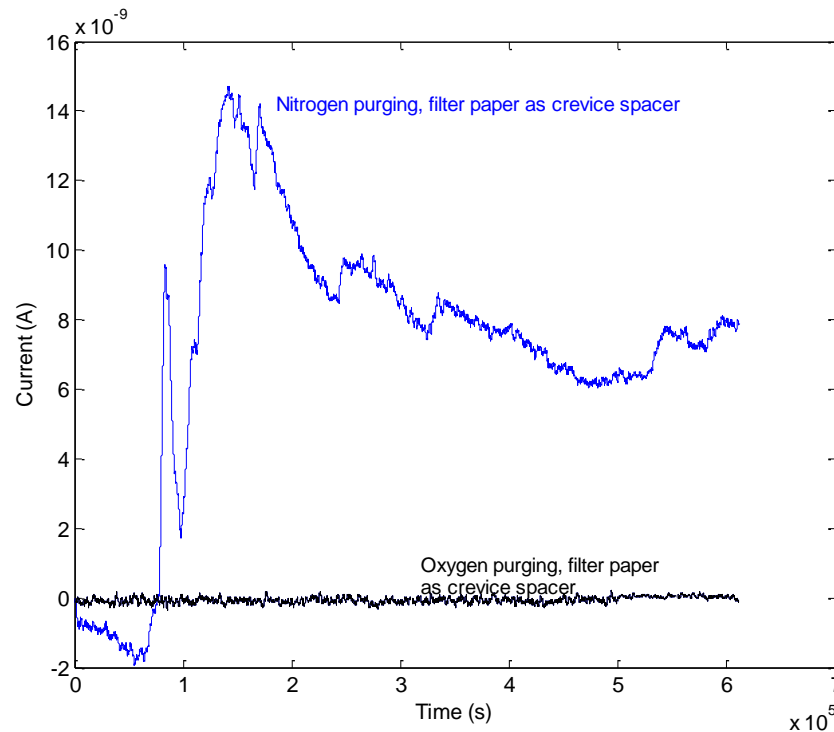
The electrochemical tests in the previous section and those reported elsewhere were performed in bulk environment. Because SCC initiation and propagation typically involves occluded geometry (e.g., crack tip) the chemistry inside the occluded geometry can be different. Thus, it is important to understand the electrochemical performance of carbon steel inside occluded regions to better understand the SCC propagation. This understanding will then in turn guide inhibitor selection for SCC control. As described earlier, the electrochemical study in the occluded geometry was achieved by performing crevice corrosion experiment on a multielectrode array.

Figure 24 shows the comparison of the current map of the array after one week of exposure at OCP in SFGE under deaerated condition (a) and aerated condition (b). Note the rectangle in the figure indicates that those electrodes were under the crevice former. Clearly, stable anodic current was seen after one week on the array exposed to deaerated solution with the anodic sites concentrated on the electrodes adjacent to the crevice mouth. In aerated solution, all electrodes showed very small magnitude of current.



**Figure 24. Current map of the array after one week of exposure at OCP in SFGE. (a) deaerated; (b) aerated (Unit: A)**

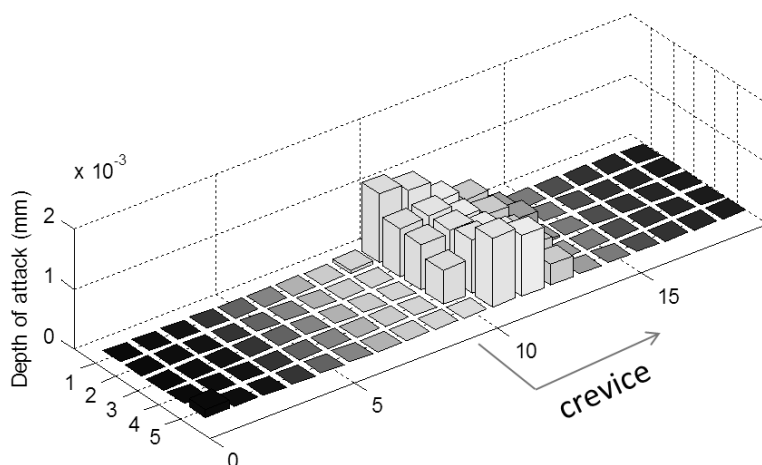
Figure 25 shows the comparison of the current of the electrode (3, 11) (row 3 and column) that is located near the crevice mouth in deaerated and aerated solutions. The difference is clear in that the electrode in aerated solution showed stable near zero current throughout the entire test duration whereas the one in deaerated condition experienced active corrosion initiation and propagation before current decay.



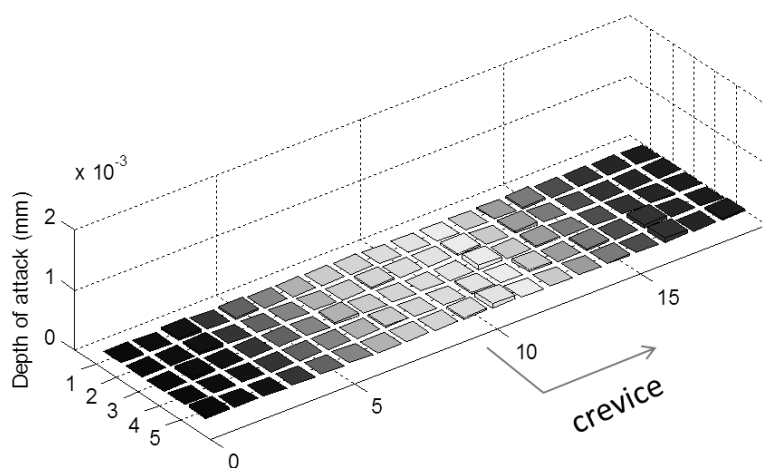
**Figure 25. Comparison of the current as a function for electrode (3, 11) that locates near the crevice mouth**

Figure 26 shows the depth of attack on the electrodes for the tests performed in deaerated and aerated SFGE. Consistent to the observation above, the electrodes in deaerated SFGE showed considerably more attack (Figure 26 (a)) than that in aerated SFGE (Figure 26 (b)).

The above results suggest that the electrochemical behavior of carbon steel inside the occlude geometry is essential the same as that in the bulk solution with respect to the role of oxygen in promoting passivity. This also may indicate that the chemistry inside the crack tip is almost identical to that in the bulk solution since the metal at the crack tip cannot be coupled with that far away from the crack tip. Such coupling would be necessary to establish potential gradient to drive the chemistry change in the crack tip as what happens in most aqueous system.



(a)



(b)

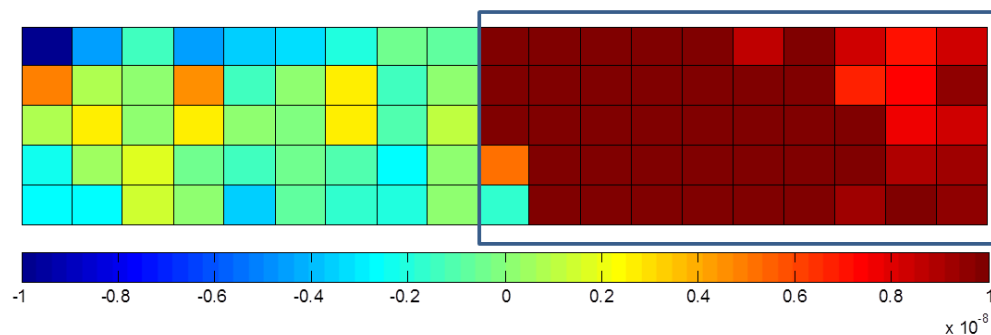
**Figure 26. Depth of attack on the electrode array after one week of immersion in SFGE at OCP . (a) deaerated; (b) aerated**



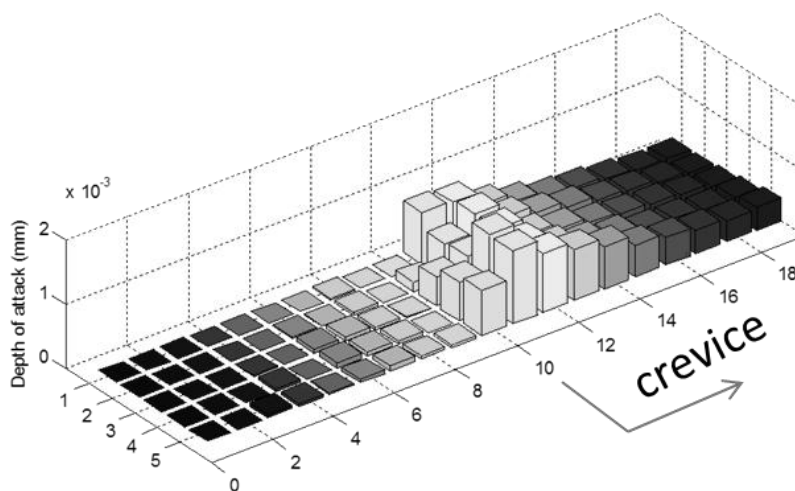
The corrosion attack in SFGE under deaerated solution seems to be driven by the potential drop (IR drop) and thus the separation of anodes and cathodes inside and outside the crevice. If there is correct, increasing the solution resistance by reducing the crevice gap (thus high IR drop) would result in shallower attack into the crevice (i.e., fewer electrodes would corrode in the crevice). In contrast, decreasing the IR drop by increasing the conductivity (adding supporting electrolyte) would result in deeper attack into the crevice (i.e., more electrodes inside the crevice would corrode).

This is confirmed by performing a test in deaerated SFGE with 0.02 M TBA-TFB as the supporting electrolyte. As shown in Figure 27, essentially all electrodes inside the crevice showed various extent of corrosion with more attack concentrated to those near the crevice mouth. A test was also performed by not using any crevice spacer thus the crevice gap would be much smaller than those shown in Figure 24. The results are shown in Figure 28. Not surprisingly, corrosion was only seen in two rows of electrodes near the crevice mouth and the depth of attack was much smaller than when the crevice spacer was used.





(a) Current map (unit: A)



(b) Depth of attack

**Figure 27. Current map (a) and depth of attack for the electrode array after approximately 90 hours immersion in deaerated SFGE with 0.02 M TBA-TFB as the supporting electrolyte.**

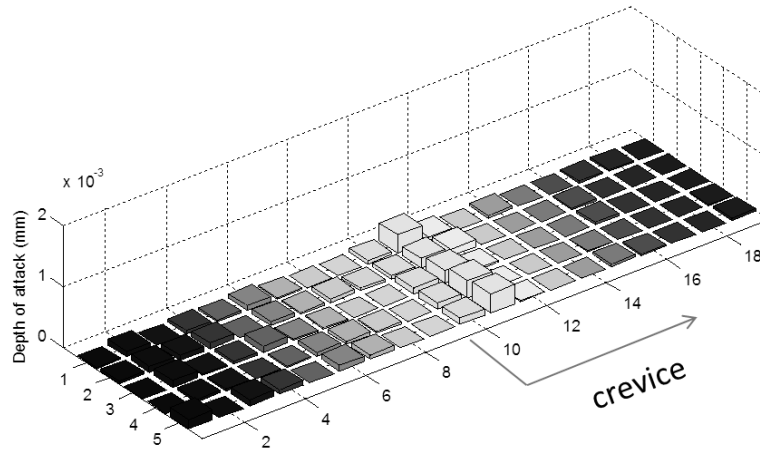
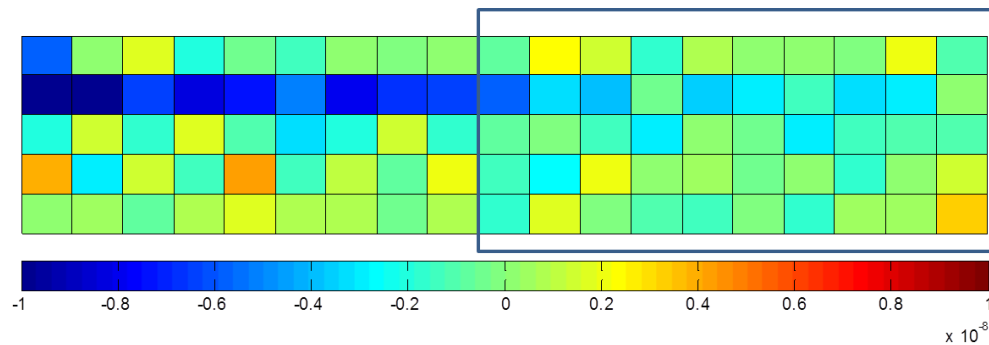


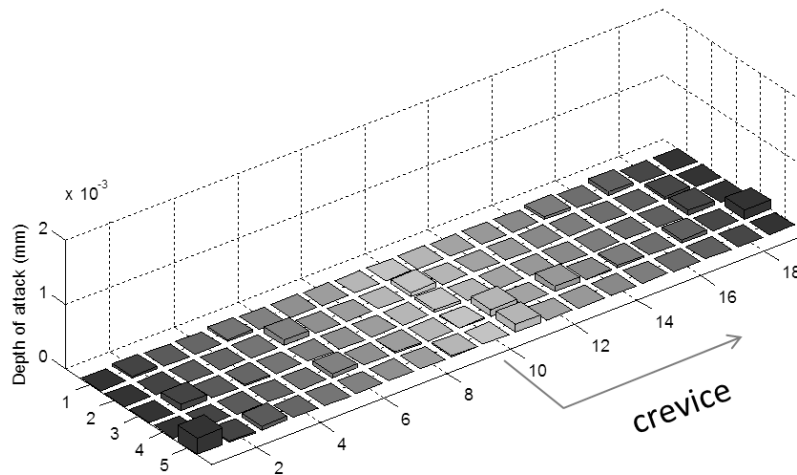
**Figure 28. Depth of attack for the array with tighter gap exposed in deaerated SFGE for one week.**

It was mentioned above that carbon steel needs the presence of oxygen in SFGE to show passivity. The electrode array certainly showed passive behavior in the solution purged by 20% oxygen (air) (Figure 24). A test was performed to investigate whether the passivity at OCP can be gained with 1% oxygen. The results are shown in Figure 29. As can be seen, the electrode array remained passive with small magnitude of current even with only 1% oxygen in the gas phase. Only minimal of attack was seen on several electrodes in the crevice over one week of exposure.

The results obtained thus far indicate that small oxygen concentration (1%) can protect carbon steel from corrosion whereas the threshold oxygen concentration for SCC in SFGE is at a much higher level (10% to 15%). This seems to confirm that the role of oxygen is not only to protect the crack wall but also to polarize the crack tip to drive the corrosion to occur. Because of this, a minimum amount of oxygen concentration is needed to maintain the polarization.



(a) Current map (unit: A)



(b) Depth of attack

**Figure 29. Current map (a) and the depth of attack for the array after one week of exposure at OCP in SFGE purged with 1% oxygen**

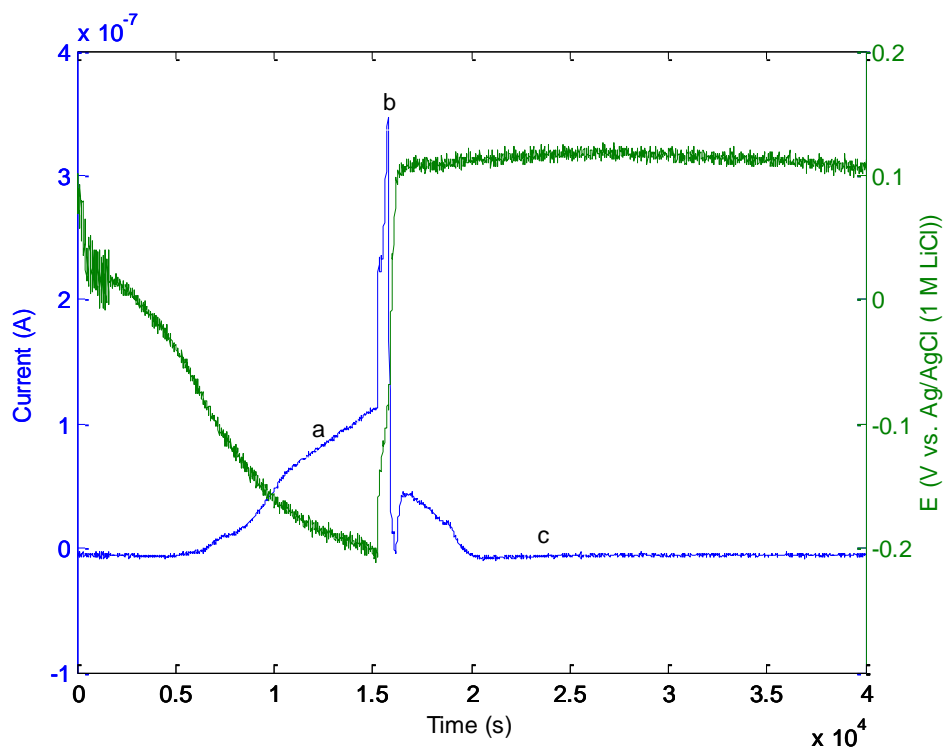
The role of oxygen in passivating the steel and driving corrosion is further illustrated in a test performed by switching the gas from nitrogen to oxygen while monitoring the current changes.

Figure 30 shows the current and potential change for electrode (3, 10) located near the crevice mouth in the test (a), the current map of the array (b) to (d) at different point of the test. The test begun in deaerated SFGE containing 0.02 M TBA-TFB as the supporting electrolyte and the purging gas was switched from nitrogen to air at the first inflection point of the potential vs. time curve shown in Figure 30 (a). Stable and active corrosion was observed on all electrodes inside

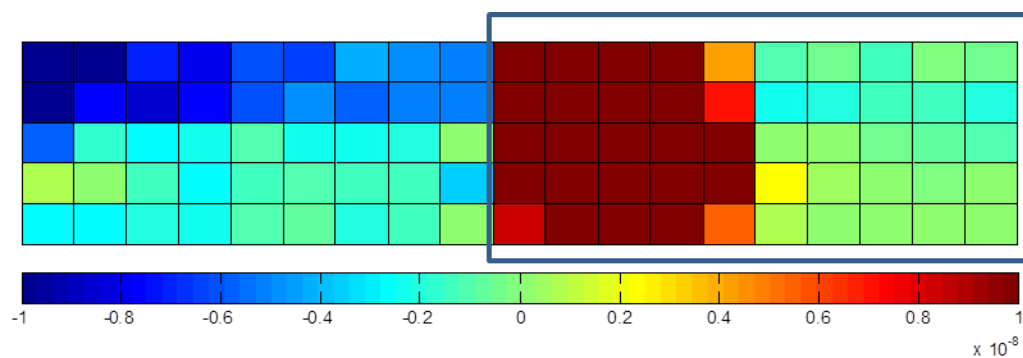
the crevice in deaerated SFGE, as shown in Figure 30 (b) when the gas was switched to air, the cathodic current magnitude increased considerably as can be seen in Figure 30 (c) since the dominated cathodic reaction is the oxygen reduction reaction. The introduction of oxygen immediately resulted in the shifting in the potential from below zero to near 0.1 V vs. Ag/AgCl. The current, in the meantime, also exhibited a spike likely due to the increase polarization from the potential shift (point b on the current vs. time curve in Figure 30 (a)). From point b, however, the current started to decay. This is very likely due to the diffusion of oxygen into the crevice to start to promote passivation of carbon steel. At point c of shown in Figure 30 (a), oxygen had penetrated into entire crevice and inhibited the corrosion initiated in deaerated condition. This is clearly shown in Figure 30 (d) by the small current magnitude on the electrode array.

These results further demonstrated the role of oxygen in promoting passivity and also provide the polarization derivation force before passive film was formed. In fact, it is not difficult to imagine that this could happen at the crack tip during the crack propagation. When the fresh metal was present due to plastic straining the presence of oxygen will first drive the metal dissolution process before passivating it until further plastic straining process to break the passive film. Thus, the SCC propagation in FGE could be a combination of anodic dissolution and film break down type of mechanism.

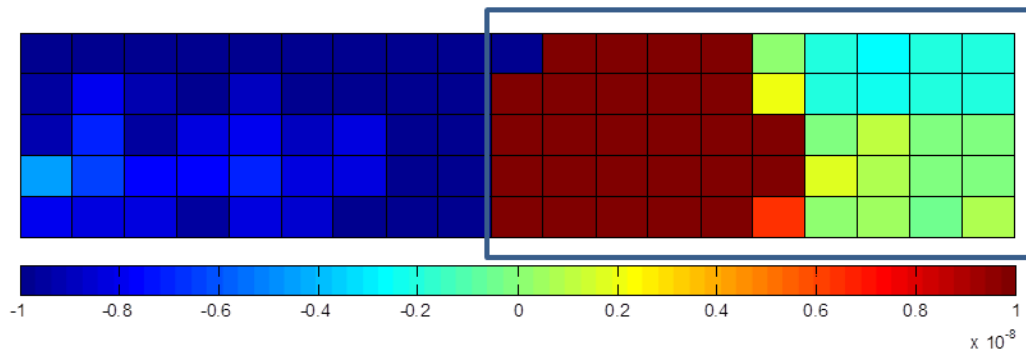
The above results not only furthered the understanding in the SCC mechanism in FGE it also supports the observation that effective inhibitors need to be able to provide corrosion protection first on the carbon steel in deaerated condition. Thus, electrochemical test should be a viable technique in the inhibitor screening before time and cost consuming crack growth rate confirmation tests.



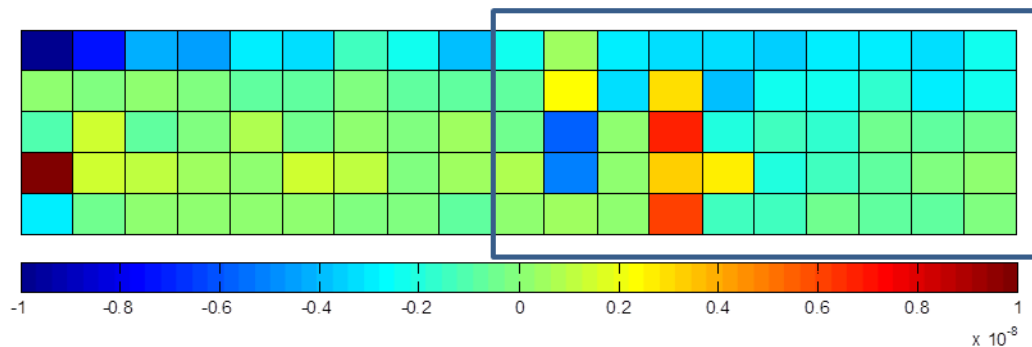
(a) Electrode (3,10) current and cell potential change vs. time



(b) Current map at point a: nitrogen purging



(c) Current map at point b: switched to air



(d) Current map at point c: oxygen passivated the propagating corrosion

**Figure 30. Current of the electrode (10, 3) at the crevice mouth and the electrode potential as a function of time in the test when the purging gas was switched from nitrogen to air. The current maps at three different points on the current of the electrode (10, 3) are shown.**

### 7.3 Task 3: Feasibility Evaluation

It has been proposed to control SCC of carbon steel in FGE by oxygen control or chemical addition. A separated project funded by PHMSA was completed in December 2011 (#WP384) to evaluate the feasibility of removing oxygen to control SCC. The major conclusion from that project was that oxygen control may not be an attractive solution when large volume of ethanol involved due to the cost and time resulted from the oxygen removal.

The results from the present project seem to suggest that chemical inhibition of carbon steel SCC in ethanol is a viable option. This is supported by the following aspects:



- Commercially available inhibitors or generic chemicals (such as  $\text{NH}_4\text{OH}$ ) selected for use in this work were all demonstrated to be able to stall the propagating crack in SFGE, FGE and E50;
- The performance of those inhibitors shown to be effective in stagnant solution remain the same under flowing condition that mimics the turbulent pipe flow;
- Electrochemical technique was able to provide fast screening of inhibitors for a specific application before confirmed by CGR tests; the results from the study of the role of oxygen and carbon steel SCC mechanism support this statement;
- The industry has established the inhibitor injection practice to control general corrosion; such practice can be easily extended to SCC control;

## 8.0 SUMMARY

These are the key results based on the performed tests:

- Commercially available inhibitors or generic chemicals (such as  $\text{NH}_4\text{OH}$ ) selected for use in this work were all demonstrated to be able to mitigate the propagating crack in SFGE, FGE and E50;
- Ammonium hydroxide was the most effective inhibitor but the addition of a minimum effective concentration would result in a pH of  $\sim 9$  that is the upper bound of the current fuel specification;
- Although some commercial inhibitors tested in this work can mitigate SCC in E50, substantially higher concentration is needed compared to when  $\text{NH}_4\text{OH}$  was used;
- The performance of those inhibitors shown to be effective in stagnant solution remains the same under flowing condition that mimics the turbulent pipe flow;
- Electrochemical technique was able to provide fast screening of inhibitors for a specific application before confirmed by CGR tests; the results from the study of the role of oxygen and carbon steel SCC mechanism support this statement;
- Chemical inhibition of carbon steel SCC in FGE is a viable option based on the obtained results. The industry has established the inhibitor injection practice to control general corrosion; such practice can be easily extended to SCC control;



---

## **APPENDIX: CGR TESTS SUMMARY TABLE**





Specimen Number	Time Period, days	R Ratio	Test Enviroment	Kmax Start-End	$\Delta K$ Start-End	Crack Growth, inches	Crack Growth Rate, mm/s	Note
HAZ-2	0-29	0.77	SFGE	33.1 - 32.8	7.6 - 7.4	0.0000	0.00E+00	Start
HAZ-2	29 - 47	0.79	SFGE	34.9 - 34.8	7.3 - 7.4	0.0000	0.00E+00	Raised Load
HAZ-2	48 - 85	0.79	E50	35.0 - 35.0	7.4 - 7.4	0.0000	0.00E+00	Changed to E50
HAZ-2	85 - 129	0.79	E50	34.8 - 34.7	7.4 - 7.4	0.0000	0.00E+00	Unload - Reload
HAZ-2	129 - 136	0.69	E50	34.3 - 37.2	10.7 - 11.5	0.0254	1.11E-06	Fast Cycling
HAZ-2	136 - 181	0.78	E50	37.4 - 38.1	8.2 - 8.4	0.0050	3.27E-08	Returned To Regular Cycling
HAZ-2	181 - 236	0.78	E50	38.1 - 38.1	8.4 - 8.4	0.0000	0.00E+00	Added 125 ppm 30% NH <sub>4</sub> OH
HAZ-2	236 - 321	0.79	SFGE	38.1 - 38.9	8.4 - 8.2	0.0069	2.39E-08	Changed to SFGE
HAZ-2	321 - 362	0.78	SFGE	38.4 - 38.5	8.5 - 8.5	0.0003	2.15E-09	Added 250 ppm INHIBITOR B
HAZ-2	362	0.78	SFGE	38.8	8.6			Changed to SFGE
	Solution was changed to SFGE on Day 362. Cracking stopped and would not reinitiate. Fast cycling was started on Day 428 and the load was increased on Day 442 and again on Day 462. Cracking was initiated and returned to regular cycling on Day 471.							
HAZ-2	471	0.81	SFGE	39		0.0042		
HAZ-2	471 -494	0.76	SFGE	39.0 - 39.3	9.4 - 9.5	0.0017	2.20E-08	Steady Cracking Established Again
HAZ-2	494 - 555	0.76	SFGE	39.3 - 39.2	9.5 - 9.4	0.0000	0.00E+00	Changed Gas to 1% O <sub>2</sub> Balance N <sub>2</sub>
HAZ-2	555 - 656	0.76	SFGE	39.2 - 39.1	9.4 - 9.3	0.0000	0.00E+00	Changed Back to Air
HAZ-2	656 - 780	0.76	E50 SFGE	39.1 - 40.1	9.3 - 11.7	0.0077	1.84E-08	Changed to E50 SFGE
HAZ-2	780 - 812	0.70	E50 SFGE	39.5 - 39.9	11.7 - 11.8	0.0034	3.12E-08	Added 250 ppm Inhibitor A, Lowered Load Slightly
HAZ-2	812 - 834	0.70	E50 SFGE	39.9 - 40.2	11.8 - 11.7	0.0038	5.05E-08	Flushed Cell Fresh E50
Base-9	45-93	0.63	SFGE	38.0 - 38.7	14.1 - 14.6	0.0061	3.74E-08	Start
Base-9	93-195	0.63	Inhibitor DEA	38.7 - 39.5	14.6 - 14.8	0.0082	2.36E-08	500 ppm DEA, Day 93
Base-9	195-243	0.63	SFGE	39.5 - 40.3	14.8 - 15.1	0.0066	4.04E-08	Flushed cell New SFGE, Day 195
Base-9	243-281	0.61	SFGE	38.6 - 39.1	15.2 - 15.3	0.0034	2.63E-08	Lowered Load, Day 243
Base-9	281-332	0.61	E50 1%O <sub>2</sub>	39.1 - 39.3	15.3 - 15.4	0.0018	1.04E-08	E50 With 1% O <sub>2</sub> , Day 281



Specimen Number	Time Period, days	R Ratio	Test Enviroment	Kmax Start-End	$\Delta K$ Start-End	Crack Growth, inches	Crack Growth Rate, mm/s	Note
Base-9	332 - 366	0.59	E50 & Air	37.2 - 37.5	15.4 - 15.6	0.0017	1.47E-08	E50 With Air - Lowered Load
Base-9	366 - 477	0.58	E50 & Air	37.5 - 37.6	15.6 - 15.4	0.0017	7.95E-09	Added 250 ppm Corr Pro 154 - Cracking Is Slowing
Base-9	477 - 603	0.59	Real FGE	34.6 - 35.4	14.1 - 14.3	0.0094	2.19E-08	Changed to Real FGE and lowered load
Base-9	603	0.60	SFGE	35.4	14.3		N/A	Changed to SFGE
	Solution was changed to SFGE on Day 603. Cracking stopped around Day 610 and would not reinitiate. Fast cycling was started and ran from Day 650 to Day 655. The crack remained dormant when regular cycling resumed. Changed to E50 SFGE on Day 713. Between Day 730 and Day 772 Load increases and fast cycling were used to reinitiate the crack. After reinitiation the load was decreased and steady cracking was established by Day 800							
Base-9	800	0.59	E50 SFGE	39.4	15.9	0.0209	N/A	E50 SFGE
Base-9	800-824	0.59	E50 SFGE	39.4 - 40.1	16.1 - 16.5	0.0053	5.02E-08	E50 SFGE
Base-9	824-869	0.59	SFGE/USW 154	40.1 - 43.0	16.5 - 17.5	0.0197	1.29E-07	250 ppm
Base-9	869-886	0.59	SFGE/USW 154	43.0 - 43.5	17.5 - 17.7	0.0029	5.01E-08	Added another 500 ppm
								Test Over
Base 10	26-68	0.66	LTV-200	33.5 - 33.4	11.3 - 11.4	0	0	Start with LTV-200
Base 10	72-80	0.61	SFGE	33.2 - 35.7	13.1 - 14.1	0.0246	9.04E-07	Changed Cycle Time to 7.63E-03Hz, Day 72
Base 10	80-131	0.61	SFGE	36.6 - 37.2	14.2 - 14.5	0.0073	4.30E-08	Changed Cycle Time Back To 1.20E-04 Htz, Day 80
Base 10	131-148	0.61	Inhibitor NH <sub>4</sub> OH	37.2 - 37.2	14.5 - 14.5	0.0006	1.04E-08	500 ppm 30% NH <sub>4</sub> OH
Base 10	148-225	0.61	SFGE	37.2 - 37.2	14.5 - 14.5	0	0.00E+00	Electrical problem No cracking after this
Base 10	225-275	0.61	SFGE	37.0 - 37.6	14.4 - 14.6	0.054	3.17E-08	Reestablished Cracking
Base 10	275-301	0.61	E50 1%O <sub>2</sub>	37.6 - 37.3	14.7 - 14.5	0	0.00E+00	E-50 1%O <sub>2</sub> Data Problem
Base 10	301 - 331	0.61	E50	37.1 - 37.7	14.5 - 14.6	0.0059	5.78E-08	Ended 1% O <sub>2</sub> Back to Air
Base 10	331 - 352	0.61	062909-1 / E50	37.7 - 39.2	14.6 - 15.2	0.0141	1.97E-07	Added 500 ppm Inhibitor 062909-1 No Effect



Specimen Number	Time Period, days	R Ratio	Test Enviroment	Kmax Start-End	$\Delta K$ Start-End	Crack Growth, inches	Crack Growth Rate, mm/s	Note
Base 10	352 - 360	0.6	Fresh E50	38.5 - 40.0	15.2 - 15.9	0.0119	4.37E-07	Flushed Cell Added Fresh E50 Lowered Load
Base 10	360 - 455	0.58	SFGE	37.8 - 38.4	15.8 - 16.0	0.0049	1.52E-08	Changed to SFGE E95 Lowered Load
Base 10	455 - 511	0.58	SFGE	38.4 - 38.6	16.0 - 16.1	0.0017	8.92E-09	Added Champion TSJ01-33-5
Base 10	511 - 597	0.58	SFGE	38.6 - 39.1	16.1 - 16.4	0.0049	1.68E-08	Flushed Cell Added Fresh SFGE
Base 10	597 - 643	0.58	SFGE	38.8 - 39.3	16.4 - 16.6	0.0056	3.58E-08	Added 1/2 Dose of Inhibitor C
Base 10	643 - 702	0.58	SFGE	39.3 - 39.9	16.6 - 16.9	0.0064	3.19E-08	Added additional 1/4 Dose of Inhibitor C
Base 10	702 - 725	0.63	SFGE	38.5 - 38.8	16.8 - 14.2	0.0021	2.68E-08	Lowered Load and Adjusted R Value
Base 10	725 - 782	0.63	SFGE	38.8 - 39.7	14.2 - 14.6	0.0091	4.69E-08	Added 62.5 ppm of 30% NH <sub>4</sub> OH
Base 10	782 - 810	0.63	SFGE	39.7 - 40.5	14.6 - 15.0	0.0680	7.14E-08	Flushed and Filled with Fresh SFGE
Base 10	810 - 834	0.62	SFGE	39.3 - 43.1	15.0 - 16.2	0.0044	5.39E-08	Lowered Load
Base 10	834 - 874	0.61	SFGE	39.3 - 40.5	15.1 - 15.6	0.0092	6.76E-08	Added 125 ppm of Inhibitor A
								End Test
Base 11	22 - 68	0.62	SFGE	34.1 - 34.9	13.0 - 13.3	0.0098	5.01E-08	Start
Base 11	68 - 126	0.62	Batching	34.9 - 34.0	13.3 - 13.2	0	0.00E+00	Batching 23 hrs. Gas 1 hr. SFGE, Day 68
Base 11	126 - 141	0.61	SFGE	34.0 - 34.0	13.2 - 13.2	0	0.00E+00	Ended Batching Left SFGE, Day 126
Base 11	141 - 159	0.62	SFGE	33.9 - 33.7	13.0 - 12.9	0.0002	3.27E-09	Unload/Reload, Day 141
Base 11	159 - 180	0.62	SFGE	34.3 - 34.2	12.9 - 12.9	0.0002	2.80E-09	Added Load, Day 159
Base 11	180 - 216	0.62	SFGE	33.7 - 34.1	12.6 - 12.9	0.0097	7.92E-08	Changed Cycle Time to 7.63E-03Hz, Day 180
Base 11	216 - 250	0.62	SFGE	35.4 - 35.6	13.7 - 13.8	0.0031	3.14E-08	Changed Cycle Time Back To 1.20E-04 Htz, Day 216
Base-11	250 - 266	0.61	E50	35.6 - 37.5	13.8 - 14.5	0.0183	3.36E-07	Changed To E50
Base-11	266 - 330	0.61	E50 / NH <sub>4</sub> OH	37.5 - 37.7	14.5 - 14.5	0.0025	1.15E-08	Added 500 ppm of 30% NH <sub>4</sub> OH
Base-11	290 - 330	0.61	E50 / NH <sub>4</sub> OH	37.6 - 37.7	14.5 - 14.5	0.0002	1.47E-09	Virtually no cracking in latter part of test
Base-11	330 - 349	0.62	E50	37.7 - 39.5	14.5 - 15.2	0.0151	2.34E-07	Fresh E50



Specimen Number	Time Period, days	R Ratio	Test Enviroment	Kmax Start-End	$\Delta K$ Start-End	Crack Growth, inches	Crack Growth Rate, mm/s	Note
Base-11	349 - 383	0.62	SFGE / 6% H <sub>2</sub> O	39.5 - 39.8	15.2 - 15.3	0.0039	3.37E-08	Changed To SFGE with 6% H <sub>2</sub> O
Base-11	383 - 423	0.60	SFGE	39.8 - 40.4	15.3 - 15.5	0.0047	3.45E-08	Fresh SFGE
Base-11	423 - 462	0.60	SFGE	37.7 - 38.0	15.2 - 15.3	0.0029	2.19E-08	Unloaded and lowered Load
Base-11	462 - 538	0.60	SFGE	37.8 - 39.2	15.1 - 15.6	0.0112	4.33E-08	Added 62.5 ppm 30% NH <sub>4</sub> OH
Base-11	538 - 585	0.59	SFGE	38.4 - 38.3	15.8 - 15.7	0	0.00E+00	Changed to SFGE, N <sub>2</sub> Gas, Lowered Load 1K
Base-11	585 - 647	0.59	SFGE	38.2 - 38.2	15.6 - 15.6	0	0.00E+00	Changed to 1% O <sub>2</sub> Balance N <sub>2</sub>
Base-11	647 - 703	0.59	SFGE	38.2 - 38.23	15.6 - 15.6	0	0.00E+00	Changed to 5% O <sub>2</sub> Balance N <sub>2</sub>
Base-11	703 - 742	0.59	SFGE	38.2 - 38.3	15.6 - 15.7	0.0009	6.78E-09	Changed to Air
Base-11	742 - 777	0.59	SFGE	38.3 - 38.3	15.7 - 15.7	0	0.00E+00	Changed to 5% O <sub>2</sub> Balance N <sub>2</sub>
Base-11	777 - 804	0.59	SFGE	38.3 - 38.9	15.7 - 15.9	0.0044	4.79E-08	Changed to Air
Base-11	804 - 857	0.59	SFGE	38.9 - 39.1	15.9 - 16.0	0.0013	7.21E-09	Changed to 10% O <sub>2</sub> Balance N <sub>2</sub>
Base-11	857 - 882	0.59	SFGE	39.1 - 39.5	16.0 - 16.2	0.0040	4.70E-08	Changed to Air
Base-11	882 - 970	0.60	SFGE	38.9 - 39.2	15.8 - 15.9	0.0250	8.26E-09	Added 880 pm Isoascorbic Acid
Base 11	970 - 1025	0.60	SFGE	39.2 - 39.2	15.9 - 15.9	0	0.00E+00	Flushed Cell Aded Fresh SFGE
Base-11								End Test
Base 12	0-121	0.61	SFGE	34.9 - 37.9	13.7 - 15.1	0.0315	7.65E-08	Start
Base 12	121 - 211	0.6	SFGE	38.1 - 38.0	15.1 - 15.0	0.001	3.59E-09	Inhibitor 500 ppm 062909-1, Day 121
Base 12	211 - 223	0.6	E50	37.2 - 38.9	15.1 - 15.8	0.0162	3.97E-07	Flushed Cell, Added E50, Lowered Load
Base-12	223 - 237	0.6	E50 + 062909-1	38.9 - 42.1	15.8 - 17.0	0.0261	5.48E-07	Added 500 ppm 062909-1
Base-12	237 - 267	0.6	E50 + 062909-1	36.6 - 38.5	14.5 - 15.2	0.0143	1.40E-07	Lowered Load
Base-12	267 - 276	0.59	SFGE	37.2 - 37.2	15.4 - 15.4	0	0.00E+00	Lowered Load and Fresh E95 SFGE
Base-12	276 - 322	0.58	SFGE	36.3 - 36.5	15.4 - 15.6	0.0017	1.09E-08	Lowered Load
Base-12	322 - 387	0.58	E50	36.7 - 39.1	15.0 - 16.4	0.0143	6.47E-08	Changed To E50



Specimen Number	Time Period, days	R Ratio	Test Enviroment	Kmax Start-End	$\Delta K$ Start-End	Crack Growth, inches	Crack Growth Rate, mm/s	Note
Base-12	387 - 429	0.58	Real FGE	39.1 - 43.3	16.4 - 18.2	0.0268	1.88E-08	Changed to Real FGE #1602553
Base-12	429 - 450		Real FGE	43.3 - 43.4	18.2 - 18.2	0.0005	7.00E-09	Added 500 pm 30% NH4OH
Base-12								End Test
Base 15	23 - 64	0.66	SFGE Flowing	35.1 - 35.5	12.0 - 12.0	0.0064	4.59E-07	Start SFGE Flowing conditions
Base-15	64 - 120	0.66	SFGE / NH4OH	35.5 - 35.5	11.9 - 11.9	0.0002	1.05E-09	Added 500 ppm of 30% NH4OH
Base-15	122 - 149	0.66	E95 SFGE	35.5 - 35.6	12.0 - 12.0	0.0034	3.70E-08	Flushed Cell Added E95 SFGE
Base-15	149 - 174	0.66	Real FGE	35.9 - 37.0	12.1 - 12.5	0.0097	1.14E-08	Changed to Real FGE #1602554
Base-15	174 - 196	0.66	Real FGE	36.5 - 37.2	12.5 - 12.7	0.0062	8.28e-o8	Added 500ppm INHIBITOR B and Lowered Load Slightly
Base-15	196 - 226	0.66	Real FGE	37.2 - 37.1	12.7 - 12.4	0.0031	3.04E-08	Added 3000 ppm MCC5201
Base-15	226 - 246							Moved Cell to New Frame
Base 15	246 - 271	0.6	E50 SFGE	32.4 - 33.8	13.0 - 13.6	0.015	1.76E-07	Changed to E50 SFGE
Base 15	271_330	0.6	E50 SFGE	33.8 - 34.8	13.6 - 13.9	0.0093	4.63E-08	Added 3000 ppm INHIBITOR B
Base 15	330 - 413	0.6	SFGE	34.8 - 35.9	13.9 - 14.2	0.0122	4.32E-08	Changed to SFGE
								Running
Base-17	5-24	0.59	SFGE	33.6 - 33.7	13.7 - 13.7	0.0057	8.82E-08	Steady Cracking
Base-17	24 - 51	0.59	SFGE	33.7 - 33.5	13.7 - 13.5	0.0004	4.36E-08	Added 250 ppm Inhibitor A
Base-17	51 - 70	0.60	SFGE	33.5 - 33.6	13.5 - 13.5	0.0165	2.55E-07	Flushed and Refilled with SFGE
Base-17	70 - 94	0.60	SFGE	33.6 - 33.6	13.5 - 13.4	0.0010	1.22E-08	Added Inhibitor C
Base-17	94 - 129	0.60	SFGE	33.6 - 34.1	13.4 - 13.6	0.0046	3.86E-08	Flushed and Refilled with SFGE
Base-17	129 - 218	0.60	SFGE	34.1 - 33.8	13.6 - 13.2	0.0047	2.09E-08	Added 500 pm INHIBITOR B
Base-17	218 - 248	0.60	SFGE	33.8 - 34.1	13.2 - 13.4	0.0013	7.21E-08	Flushed and Refilled with SFGE
Base-17	248 - 279	0.61	FGE	34.1 - 34.1	13.4 - 13.3	0.0021	1.94E-08	Flushed and Refilled with FGE



Specimen Number	Time Period, days	R Ratio	Test Enviroment	Kmax Start-End	$\Delta K$ Start-End	Crack Growth, inches	Crack Growth Rate, mm/s	Note
Base-17	279 - 302	0.61	FGE	34.1 - 34.2	13.3 - 13.3	0.0005	6.39E-08	Added 500 ppm INHIBITOR B
								Running
Base-20	48 - 77	0.66	SFGE	33.9 - 33.9	11.4 - 11.4	0.0006	6.08E-09	Established Steady Cracking
Base-20	77 - 130	0.67	SFGE	34.4 - 34.3	11.4 - 11.2	0.0012	6.66E-09	Raised Load
Base-20	130 - 162	0.67	FGE	34.3 - 34.5	11.2 - 11.3	0.0160	1.47E-08	Changed to FGE
Base-20	162 - 185	0.67	FGE	34.5 - 34.6	11.3 - 11.3	0.0008	1.02E-08	Added 500 ppm INHIBITOR B
								Running



## Det Norske Veritas

Det Norske Veritas (DNV) is a leading, independent provider of services for managing risk with a global presence and a network of 300 offices in 100 different countries. DNV's objective is to safeguard life, property and the environment.

DNV assists its customers in managing risk by providing three categories of service: classification, certification, and consultancy. Since establishment as an independent foundation in 1864, DNV has become an internationally recognized provider of technical and managerial consultancy services and one of the world's leading classification societies. This means continuously developing new approaches to health, safety, quality and environmental management, so businesses can run smoothly in a world full of surprises.

## Global Impact for a Safe and Sustainable Future

Learn more on [www.dnv.com](http://www.dnv.com)